

# The Power of Silk Technology for Energy Applications

Stephen Strassburg, Shakir Zainuddin, and Thomas Scheibel\*

Silk fibers are a remarkable material made of proteins possessing excellent mechanical properties that match or even outperform, in some aspects, high performance fibers such as Kevlar and steel. Silk proteins can be further produced recombinantly, allowing the possibility for genetic modification, enhancing silks' already impressive range of benefits. Thus far, little research has explored the possibility of incorporating silk-based materials in electronic or energy systems. With an increasing global concern for climate change and the dwindling reserves of fossil fuels, silk (or silk-derived) hybrid materials are a promising avenue of scientific exploration in energy storage and conversion devices, flexible and wearable electronics and even as photovoltaic devices, which will be reviewed here within. Despite this, silk has seen only little interest for applications in hybrid energy devices in the recent years. Here within, some of the applications and benefits of silk-based materials in several systems including: flexible electronics, thermal and thermoelectric devices, mechanical energy devices, sensors, and photovoltaic solar cells are examined. In addition to biocompatibility, high tensile strength, and renewability, silk also adds many benefits to hybrid energy systems such as tunability, multifunctionality, and versatility, making silk one of the most all-encompassing materials for use in hybrid devices.

## 1. Introduction

The energy demands that support modern industries and lifestyles are largely fulfilled by the burning of fossil fuels,<sup>[1]</sup> whose greenhouse gas by-products are a major contributing cause of global warming.<sup>[2]</sup> It has become clear that the combustion of fossil fuels at the current scale is unsustainable and more sustainable alternative energy sources must be explored to offset the contribution of fossil fuels.<sup>[3]</sup> Solar energy has an important role to play in this transition. Solar irradiation available on Earth's surface per hour far exceeds the annual global energy demand.<sup>[4]</sup> However, adaptation to solar energy has been slow due to a number of factors, such as rare or hazardous raw materials, high sensitivity to water, and short life spans.<sup>[5]</sup> Compared to the fossil fuel, which can be burned on demand, solar irradiation is subject to fluctuations caused by many factors such as weather conditions, time of the day, time of the year, and latitude.<sup>[6]</sup>

Because storing solar radiation in its original form, that is, electromagnetic waves, is prohibitively difficult, its conversion prior to storage is necessary. Biological systems developed 3.5 billion years ago<sup>[7]</sup> as a process to use sunlight to drive chemical reactions through photosynthesis. Specifically, oxygenic photosynthesis, which occurs in most plants, algae, and cyanobacteria, converts carbon dioxide from the atmosphere into carbohydrates. These carbohydrates form dense and portable packets of chemical energy that can be released through cellular respiration whenever needed.

The first step in following nature's example in turning light energy to chemical energy was enabled with the discovery of the photovoltaic effect by Edmond Becquerel in 1839,<sup>[8]</sup> in which the current generated by an electrochemical cell increased upon exposure to light. The first photovoltaic cells in the 19th century were based on pure metal species and exhibited low efficiencies.<sup>[9]</sup> Major efficiency improvements came in the 20th century with the incorporation of semiconductor materials into photovoltaic cells but they remained bulky and difficult to manufacture.<sup>[9]</sup> A breakthrough came in the 1980s with the advent of thin film solar cells which largely solved this problem.<sup>[9]</sup> Despite many advances, solar cells have a limited lifetime, and once their efficiencies have dropped to a no longer useful level, disposal becomes an issue due to the difficulty of recycling component materials. In addition, energy storage is often a major concern due to the limited number of hours per day photovoltaic devices are exposed to solar irradiation. Thus,


S. Strassburg, S. Zainuddin, Prof. T. Scheibel  
Department of Biomaterials  
Universität Bayreuth  
Prof.-Rüdiger-Bormann-Straße 1, 95447 Bayreuth, Germany  
E-mail: thomas.scheibel@bm.uni-bayreuth.de

Prof. T. Scheibel  
Bayreuth Center for Colloids and Interfaces (BZKG)  
Universität Bayreuth  
Universitätsstraße 30, 95440 Bayreuth, Germany

Prof. T. Scheibel  
Bayreuth Center for Molecular Biosciences (BZMB)  
Universität Bayreuth  
Universitätsstraße 30, 95440 Bayreuth, Germany

Prof. T. Scheibel  
Bayreuth Center for Material Science (BayMAT)  
Universität Bayreuth  
Universitätsstraße 30, 95440 Bayreuth, Germany

Prof. T. Scheibel  
Bavarian Polymer Institute (BPI)  
Universität Bayreuth  
Universitätsstraße 30, 95440 Bayreuth, Germany

 The ORCID identification number(s) for the author(s) of this article can be found under <https://doi.org/10.1002/aenm.202100519>.

© 2021 The Authors. Advanced Energy Materials published by Wiley-VCH GmbH. This is an open access article under the terms of the Creative Commons Attribution-NonCommercial License, which permits use, distribution and reproduction in any medium, provided the original work is properly cited and is not used for commercial purposes.

DOI: 10.1002/aenm.202100519

in addition to solar energy, the development of new energy storage methods as well as alternative energy sources is vital in replacing fossil fuels.

Alternative energy sources can be broken down into roughly three categories, mechanical, thermal, and chemical energy conversion. For each of the above sources, there is a myriad of different material properties necessary, ranging from anisotropic crystalline materials for piezoelectric devices<sup>[10]</sup> or highly light-absorbent materials for light-to-heat conversion<sup>[11]</sup> to binding specificity for chemical conversions.<sup>[12]</sup> More recently, conjugated polymers, macromolecules which behave as semiconductors, are most commonly used to produce organic energy devices. These conjugated polymers are lightweight and flexible<sup>[9]</sup> and can be easily processed into various shapes including thin films (in the  $\mu\text{m}$  range)<sup>[13]</sup> but often lack the versatility—a material that is good for one particular energy conversion application is likely to be ill-suited for another. While providing a good starting point for polymer-based energy conversion systems, most of these conjugated polymers are derived from oil. With fossil fuels projected to deplete within the coming decades, including an estimated end of oil and gas production by 2066 and 2068, respectively, and of coal by 2126,<sup>[14]</sup> it is imperative that alternative, renewable, robust material sources are found.

The long-term development of organic energy conversion and storage devices must rely on biopolymers, whose raw materials can be produced in a sustainable manner. “Green” biopolymers are showing much potential in replacing at least some of the roles that fossil fuel-based polymers have dominated for the past sixty years. Nature-derived biopolymers fall into three categories: proteins/polypeptides, polysaccharides, and nucleic acids. Among these three, polysaccharides are the most abundant. For example, chitin, the primary component of exoskeletons of arthropods, crustaceans and insects, and cellulose, the primary component of algae, green plants and wood are the most abundant organic polymers on Earth.<sup>[15]</sup> Both materials have seen a plethora of recent literature on their use in thin films and energy storage devices.<sup>[16]</sup> However, despite their abundance, both polysaccharides are difficult to process, often requiring harsh chemical solvents for dissolution and they lack many of the motifs and secondary structures that can be found in proteins which limits their versatility.

Proteins/polypeptides are arguably the most diverse class of biopolymers, varying in size and function. Smaller sized proteins/polypeptides play a large role as, for example, hormones and signaling molecules, while larger proteins form, for example, enzymes, transport or structural elements.<sup>[17]</sup> They can be harvested from plants and/or animals, produced recombinantly and offer many tunable/variable amino acid sequences and motifs

One well-known protein-based material is silk. While silk fibers have long been associated with luxury textiles, silk-based materials are now being researched intensively for applications in various technical and medical fields. Silk fibers can be dissolved, and the solvated proteins processed into many different morphologies such as films, foams, gels, particles, capsules, and nanofibers.<sup>[18]</sup> Such silk morphologies can play a role as scaffolds in tissue engineering,<sup>[19]</sup> drug delivery systems in medicine,<sup>[20]</sup> and particle filter enhancer in air filtration.<sup>[21]</sup> Apart from being functionally diverse, silk also possesses good mechanical properties,<sup>[22]</sup> is biodegradable<sup>[23]</sup> and biocompat-

ible,<sup>[24]</sup> and some species even produce bacterial repellent strains.<sup>[25]</sup> Even though it lacks inherent photocatalytic or photovoltaic activity, silk is a material that can be easily modified or blended in composites or even carbonized into conductive materials. It is then no surprise that more and more literature is appearing examining silk for use in a wide range of photovoltaic and green energy devices.

Here within, we review the literature on silk processing, the applications of silk in the rising field of flexible electronics, and the application of silk in several green energy conversion systems, which points to the potential of silk being incorporated into solar energy conversion devices.

## 2. Silk and Processing of Silk Proteins

Much of the knowledge pertaining to silk processing developed from the textiles industry. Though certain cultures developed their own unique uses of silk from various wild species,<sup>[26–28]</sup> their scale of production remained small and never came close to that of the domesticated silk moth, *Bombyx mori*, which for millennia centered in China.<sup>[29]</sup> The high availability of *B. mori* silk is the result of the evolutionary luck (or misfortune) of wild moths, which happened to be the species whose larvae spun cocoons that humans thousands of years ago found useful and ended up being domesticated and shaped into the modern *B. mori* strain.

However, more recent examinations have looked at the silk from other, hitherto less generous sources such as spiders,<sup>[30]</sup> lacewings,<sup>[31]</sup> and bees<sup>[32]</sup> (Figure 1a). At a macromolecular level there are similarities and differences between the silks from various arthropods.<sup>[33]</sup> For example, spider dragline silk and silkworm silk differ in their hierarchical organization as illustrated in Figure 1b. The spider fibroin (also called spidroin) fibrils are packed into a single core sheathed in layers of glycoprotein and lipids, while the silkworm fibroin fibrils are packed into two parallel cores, sheathed by another protein called sericin. At a molecular level, silk fibroins from differing species are all made of long chains of similar amino acid sequences (though the exact sequence likely is different). Due to specific interactions between their amino acid side-chains, various secondary structures such as random coils,  $\alpha$ -helices, and  $\beta$ -sheets are formed which are responsible for silk's high degree of crystallinity (Figure 1c). For more in-depth understanding of the secondary structure variations between different silk proteins produced by various species, we refer to a review paper by Aigner et al.<sup>[33]</sup>

The high degree of crystallinity that is found in the silk of silk-producing species is necessary for the continuous spinning of solid silk fibers out of aqueous silk solutions contained in silk glands.<sup>[34]</sup> Various silk types have therefore evolved to converge upon high crystallinity, even though their secondary structure (and amino acid sequence) differ from each other. For example, silks from certain insect species such as bees, ants, and hornets achieve high crystallinity using a high percentage of  $\alpha$ -helices that coil around each other to form coiled coil conformations,<sup>[35]</sup> while silks from other species such as the silkworm and spiders achieve this using a high percentage of  $\beta$ -sheets that pack together into crystallite units.<sup>[36]</sup> In addition, the spinning processes for many silk spinning species are often similar. This is likely another evolutionary convergence

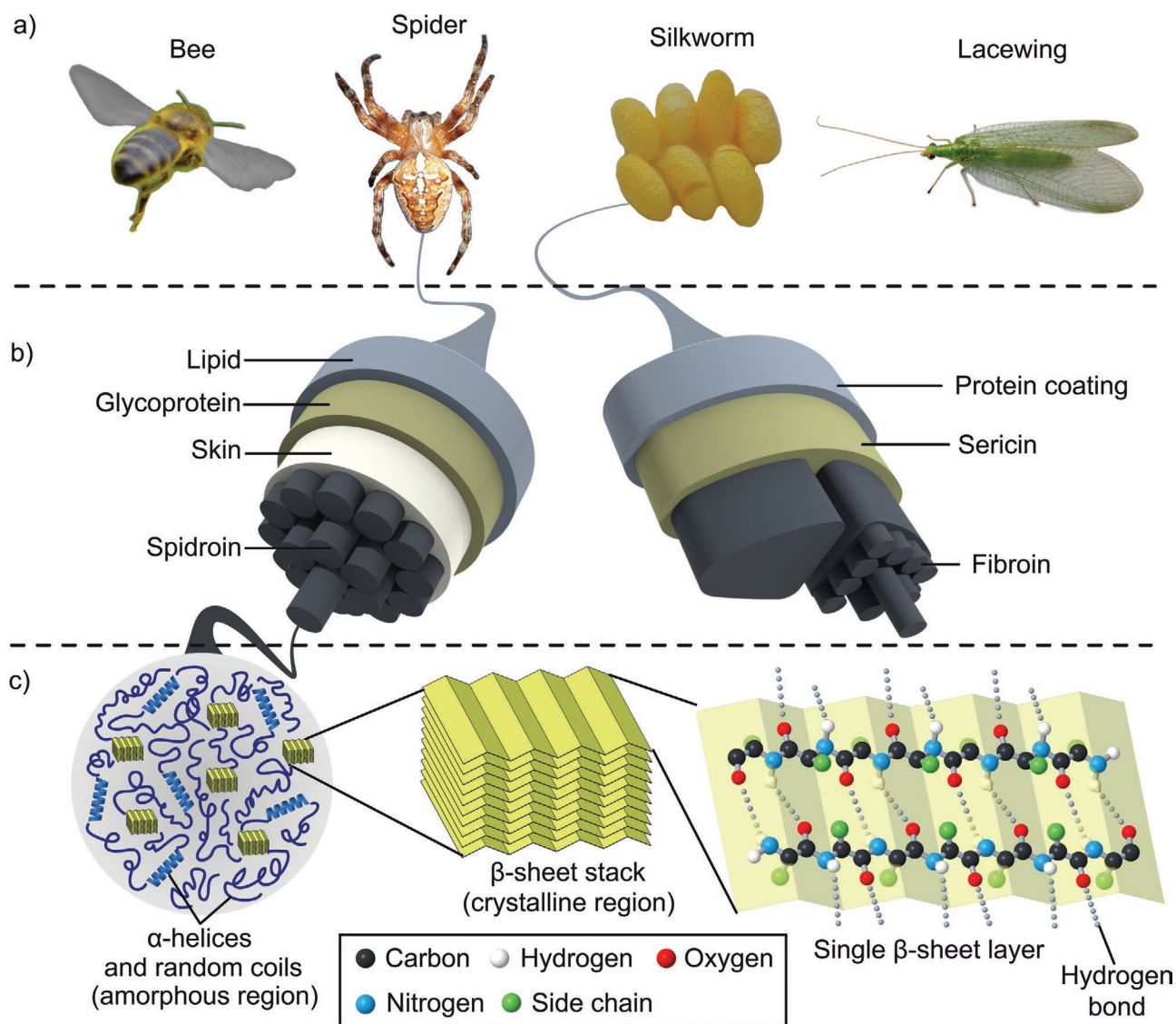


**Figure 1.** a) Pictures of natural sources of silk. b) Cross section illustration comparing the different hierarchical structures of fibers from the spider *Araneus diadematus* and the silkworm *B. mori*. c) Schematics of the secondary structures of silk which are responsible for silk's excellent mechanical properties. Silk's elasticity is attributed to the amorphous regions ( $\alpha$ -helices and random coils), whereas its rigidity is attributed to the crystallinity ( $\beta$ -sheets).

because during the spinning process, the fibroin molecules are subjected to shear along the direction of spinning, causing molecular alignment lengthwise and allowing overlapping crystalline regions to join together to form crosslink points, thus forming fibrils. The fibrils can in turn be packed together in a parallel fashion to form bundles. This hierarchical organization enables the formation of continuous strands much longer and thicker than the constituent molecules. This high degree of crystallinity, derived from secondary structures as well as spinning conditions which are similar between the different silk spinning organisms, largely accounts for the mechanical and chemical stability of silk.<sup>[37]</sup>

The dissolution of silk is a redispersion of individual silk fibrils. By using solvents that effectively denature protein, the physical crosslink points found in the crystalline region

of silk can be unmade and the continuous fiber is unfolded to its individual fibroin molecules. The dissolved protein can then be processed using techniques such as wet spinning,<sup>[38]</sup> electrospinning,<sup>[38]</sup> gelation,<sup>[39]</sup> film casting,<sup>[40,41]</sup> or particle formation<sup>[20]</sup> (Figure 2). Each of these techniques allows for the silk fibroins to be processed into new solid morphologies depending on the process used.

The morphologies of processed silk can differ in size, ranging from a few nanometers to several meters, and also in dimension, with particles, fibers, films, and gels being examples of 0-, 1-, 2-, and 3D silk-based objects, respectively. For example, submicro- and nanoparticles that can be used in drug delivery systems have been processed using precipitation yielding a range of 80–600 nm particles.<sup>[20]</sup> Spinning methods, such as electrospinning and wet spinning, enable

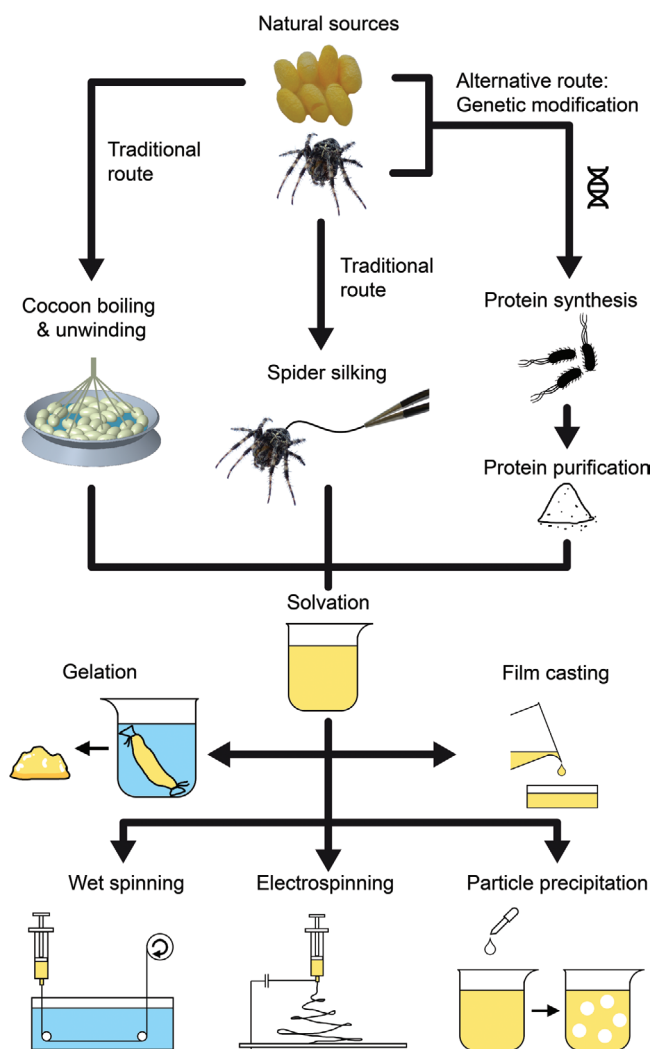


**Figure 2.** Schematic “tree” of silk processing. Silk can be obtained directly from animals, for example through harvesting of silkworm cocoons or silking of spiders. Alternatively, silk can be produced recombinantly through biotechnological techniques, for example using bacteria as host. Once the silk proteins have been obtained, they can then be solvated, which then leads to a myriad of ways of processing the silk proteins into gels, films, fibers, particles, etc.

the production of silk fibers with a wide range of diameters in the nanometers<sup>[38]</sup> and hundreds of micrometers<sup>[42]</sup> range, whereas natural silk fibers typically show a single digit to tens of micrometers diameter range.<sup>[43]</sup> Film casting methods such as spin coating and drop casting produce silk films with thickness in the nanometers to micrometers range.<sup>[40,41]</sup> Porous scaffolds of sizes ranging between 15 to 200  $\mu\text{m}$  can be produced using salt leaching<sup>[44]</sup> Under the influence of environmental factors such as temperature, pH, and salt concentration, aqueous silk solutions exhibit self-assembling behavior which can lead to the formation of hydrogels<sup>[39]</sup> and particle formation used for drug encapsulation and delivery.<sup>[20]</sup> These are but a few of the many ways for different morphologies of silk to be produced and many more examples are covered more exhaustively in other reviews.<sup>[45]</sup>

Millennia of sericulture driven by consumer demand ensured the abundance of silkworm silk. However, advances in genetic engineering have enabled the decoupling of silk production from their original animal sources, allowing silk to be produced recombinantly in a more controlled, compact, and sterile manner in simple host organisms such as bacteria or fungi. Recombinantly produced silk additionally avoids one of the major draw backs of silk as a material, namely harvesting. Spider silk for example is quite difficult to harvest due to how territorial spiders tend to behave.<sup>[46]</sup> Of course, the use of genetic engineering also adds many benefits to protein production, most notably a means to modify the silk according to the requirement of the application. Many variations of silk fibroins based on the blueprints from several spider species, such as *Nephila clavipes* or *Araneus diadematus*, have been created. This includes the changing of the residual electric charge of the protein,<sup>[47,48]</sup> the introduction of protein sequences that fluoresce,<sup>[49]</sup> show affinity for specific cells types,<sup>[50,51]</sup> and bind specific chemical species.<sup>[52,53]</sup> The introduction of artificial binding sites on the proteins permits the formation of composites and hybrids which change the property of silk well beyond mere aesthetics as had been done with dyes for millennia.<sup>[54,55]</sup> This is highly relevant as an interest in organic–inorganic hybrids is growing in recent years due to the potential of combining the various functionalities of inorganic materials with the useful properties of silk such as good processability, excellent mechanical properties, being light weight, and biocompatibility. This opens up the possibility for novel energy conversion devices that are easy to manufacture, are durable and can be applied in new ways such as in an aquatic environment or in vivo. As will be shown in various examples in the coming chapters, silk is in a good position to place itself as a key polymer in bridging the gap between sustainable materials and sustainable energy conversion.

### 3. Applications of Silk-Based Materials for Flexible and Wearable Electronics

Silk’s use in the textile industry makes it a promising fibrous material for wearable or flexible electronic materials, and several studies exist on silks as a material for flexible electronics,<sup>[56–59]</sup> electronic textiles,<sup>[60,61]</sup> and wearable sensors.<sup>[62,63]</sup> Below are a few of the more interesting applications of fibrous as well as other morphologies of silk in electronic materials.

#### 3.1. Silk Materials in Flexible Electronics

Most of literature that focuses on deformable electronics is based on synthetic polymers such as polydimethylsiloxane (PDMS), polyurethane (PU), or polymerized ionic liquids.<sup>[64–67]</sup> While these studies show promising results for flexible electronics, they often do not consider the environmental impact of using oil-based materials. For greener, biocompatible flexible electronics, silk remains a promising, but as of yet, not sufficiently examined material.

Perhaps one of the earliest studies, a study by Kang et al. in 2007, successfully obtained electrically conducting silk-carbon

nanotube hybrid non-woven membranes via electrospinning. *B. mori* silk nanofibers were first dissolved in an aqueous polyethylene oxide solution and then electrospun. The resulting nonwoven mesh was post-treated by submersion in methanol to induce  $\beta$ -sheet formation. After the conformational change, the nonwoven mesh was submerged in an aqueous multiwalled carbon nanotube (MWCNT) dispersion. The MWCNT showed strong adhesion to the highly porous silk nonwoven, and after subsequent post-treatment with deionized water a conductivity of  $2.4 \times 10^{-4} \text{ Scm}^{-1}$  was achieved.<sup>[68]</sup> The combination of high conductivity and strong adhesion between the MWCNT and nonwoven silk mesh offered the first significant advancement in the development of silk-based flexible materials.

Following initial work with silk-hybrid flexible electronics, other studies looked at ZnO nanorod arrays arranged on silk protein substrates,<sup>[57]</sup> CdS nanostructures embedded in a silk matrix,<sup>[56]</sup> and Ag nanowires embedded in silk fibroin films.<sup>[59]</sup> Each of these studies illustrated a different methodology for using silk as a material for flexible electronics.

Gogurla et al. produced photodetectors by aligning ZnO nanorod arrays on *B. mori* silk fibroin films doped with Au nanoparticles. The Au-silk substrate was then seeded with a layer of ZnO by magnetron sputtering at 100 °C, a process that had a low enough temperature to not denature or destroy the silk substrate. After sputter coating, growth of the ZnO nanorods was induced using zinc nitrate hexahydrate and hexamethylenetetramine at a temperature of 90 °C. The resulting device was flexible and showed a high photoresponse for both ultraviolet (UV) and visible wavelengths. In addition, the flexible photodetectors showed no change in performance even at different bending angles suggesting good long-term mechanical stability. The photoresponses of the devices also showed similar responses on the Au-silk substrates as it did for glass, making the silk-hybrid device a promising candidate for self-powered bio-photonics devices.<sup>[57]</sup>

Bera et al. used a similar strategy of embedding nanostructures (in this case CdS nanocrystals) in a *B. mori* silk matrix. The authors successfully demonstrated that MWCNT with added CdS nanostructures could be mixed with a silk protein solution. The MWCNT-CdS/silk solution could then be cast on chemically etched indium titanium oxide (ITO) glass and a polyethylene terephthalate (PET) substrate. The device, however, exhibited properties of a semiconductor only with the addition of CdS nanoparticles together with the MWCNT acting as an enhancement material for conductivity.<sup>[56]</sup> The silk hybrid device was successfully used as a flexible floating gate memory showing that *B. mori* silk based materials might be an attractive material for biocompatible flexible flash memory devices.

Qi et al. embedded Ag nanowires in a *B. mori* silk film for use as wearable flexible conductive textiles. The Ag nanowire solution was spin-coated on a silicon wafer and then sputtered with platinum. After sputter coating, a silk fibroin solution was drop cast on the coated Ag nanowire wafer. The Ag-nanowire silk film was then removed after drying. The resulting substrate demonstrated excellent transmittance and conductivity compared to both hard and flexible substrate controls. Furthermore, the desired transmittance and conductivity properties were retained even after prolonged stress making indicating a flexible stable device even after repeated stress cycles.<sup>[59]</sup>

A more recent paper by Shi et al. used Ag nanoparticles and bovine serum albumin (BSA) solvated in aqueous solutions with the addition of NaBH<sub>4</sub> to form Ag nanocluster-BSA complexes (AgNCs@BSA). The AgNCs@BSA were then mixed with a *B. mori* silkworm silk solution after which an ITO substrate was immersed into the blended solution allowing for the AgNCs@BSA-silk solution to adhere to the surface and act as a switching layer for a flexible bio-memristor (Figure 3a).<sup>[69]</sup> The device showed the overall best switching performance among several organic materials with a fast switching speed of 10 ns, low-power switching voltages ( $V_{\text{set}} \approx 0.3 \text{ V}$ ,  $V_{\text{reset}} \approx -0.18 \text{ V}$ ) and high switching resistance ratio. Perhaps most interesting of the authors' results is that the memristor can act as a synoptic synaptic emulator. When the AgNCs@BSA-silk-ITO device was modeled similar to that of a neuron (pulses of  $\pm 1.5 \text{ V}$  and 50 ns switching) the behavior mimics the characteristics of a biological synapse. After 800 continuous pulses (a series of 10 negative pulses followed by 10 positive pulses) or 40 cycles, the memristor performance remained unchanged indicating a good stability and reliable emulation with potential applications with synthetic synapses (Figure 3b–d).<sup>[69]</sup>

Each of the above examples uses a similar methodology for production of different silk-hybrid energy devices and highlights the versatility of silk as a substrate, matrix, film, etc. for embedding electronically conductive materials for flexible devices. All of the above examples use fillers, such as nanoparticles or MWCNT, as the conductive material which silk is uniquely adept at binding without the need of a bonding agent. In addition, as demonstrated by Shi et al, combining these conductive fillers with other proteins only enhances their compatibility with silk. With recent advances in fabrication of conductive nanocomposite silk films,<sup>[70]</sup> the specificity of silk binding motifs<sup>[52]</sup> and myriad of different types of spider silks, insect silks, and crustacean silks to choose from, there is a large number of untapped potential of silk materials for future flexible electronics.

### 3.2. Silk Textiles with Integrated Electronics

Concerning textile electronics, an early study demonstrated that *B. mori* silk fibers can be incorporated into integrated electronics as the active component of electrochemical transitions (in addition to their role as a structural component).<sup>[71]</sup> The silk fibers were stained with poly(4-(2,3-dihydrothien[3,4-b]-[1,4]dioxin-2-yl-methoxy)-1-butananesulfonic acid (PEDOT-S), a conductive conjugated polymer. The staining process was rapid, requiring only 1 h of soaking in 10 gL<sup>-1</sup> PEDOT-S solution at pH 2 and 90 °C. The dyed silk fibers could then be arranged into flexible electronic transitions with the addition of the ionic liquid 1-butyl-3-methylimidazolium bis(trifluoromethane sulfonimide), [BMIM][Tf<sub>2</sub>N], and polymerized ionic liquid poly(1-vinyl-3-methylimidazolium bis(trifluoromethane sulfonimide)), poly[ViEtIm][Tf<sub>2</sub>N]. Fibers could then be manually woven into non-conductive silk threads while still retaining similar young's moduli to undyed silk fibers. The resistances along the threads were high, a problem the authors admitted must be addressed, but this study marks an important first step towards the realization of silk-based electronic textiles and flexible organics.<sup>[71]</sup>

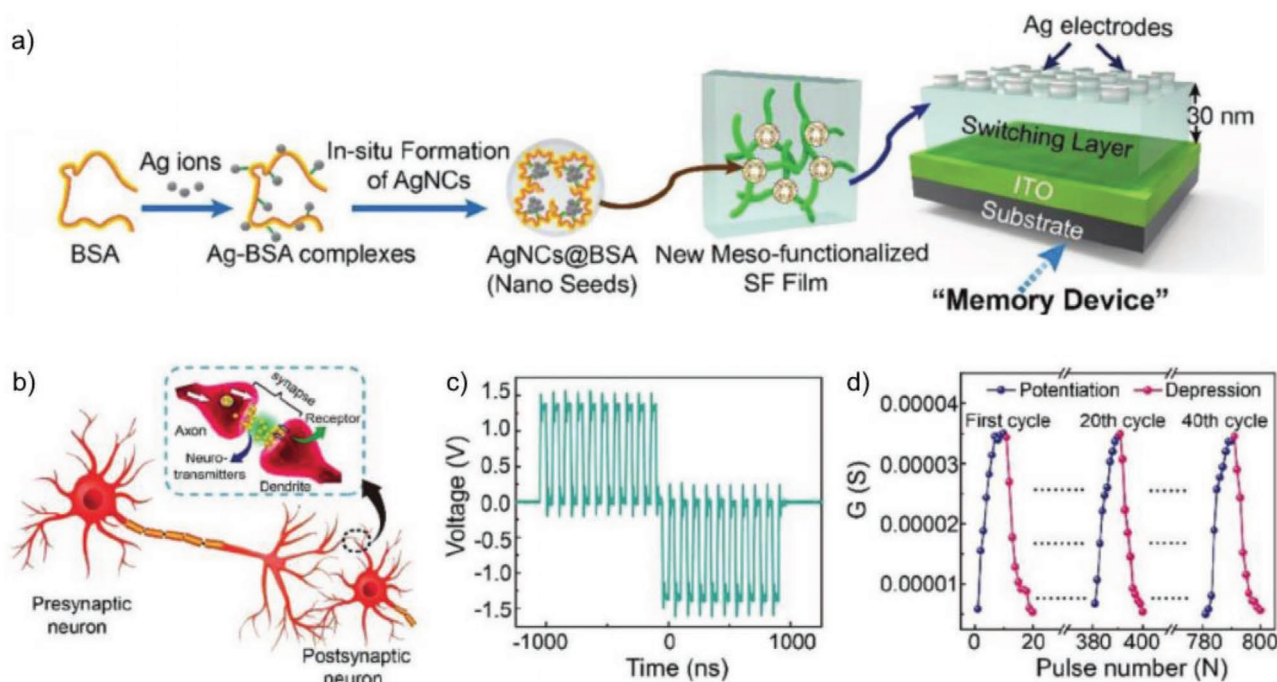


**Figure 3.** a) Schematic of the device fabrication process of a silk hybrid memristor. BSA is mixed with Ag nanoparticles to form Ag-BSA complexes which eventually form nanoclusters (AgNCs@BSA). The AgNCs@BSA nanoclusters were added to a silk solution creating a blend followed by the submersion of an ITO substrate. The blended silk-AgNCs@BSA solution was then deposited on the ITO substrate and could then be used as a switching layer of the memristor. b) Schematic representation of a neuron and structure diagram of a chemical synapse. c) A single cycle of test pulses with 10 pulses consisting of +1.5 V followed by 10 pulses of -1.5 V. d) Repeated potentiation and suppression of a silk hybrid memristor. Each cycle (10 positive, 10 negative pulses) mimics that of biological synapse with no response degradation indicating good synaptic stability.<sup>[69]</sup> Copyright 2019, Wiley.

Follow up research has seen the advent of silk composite fibers with PEDOT:PSS,<sup>[60]</sup> CNT<sup>[72]</sup> and carbon nanofillers-polyurethane matrices.<sup>[73]</sup> In each of the above cases, silk was used in conjunction with an electrically conductive material. Each study successfully showed novel ways to produce silk textiles that were electrically conductive. Perhaps the study that best summarized the robust nature of silk is the 2015 paper by Narayanan et al. The authors successfully used carbon nanofillers such as graphite, nanographite, carbon nanotubes, and carbon nanofibers dispersed in thermoplastic polyurethane, which could then be used as coatings of commercial cotton and silk textiles.<sup>[73]</sup> The silk-coated fibers were over six times more conductive than the cotton fibers; as a result the authors attributed to the large void fraction present ( $\approx 12\%$ ) in pure cotton yarn.<sup>[73]</sup> This success of fabrication and higher conductivity of silk coated fibers begins to outline the benefits of silk hybrid materials for wearable electronic applications.

The benefits of silk textiles over other biopolymer fibers also extend to processing conditions. Preparation of conductive silk fibers often only requires water, dimethyl sulfoxide, or alcohol resulting in conditions that are relatively safe or have low environmental impact.<sup>[61,74,75]</sup> Silk, also has a high degradation temperature<sup>[76–78]</sup> and can be pyrolyzed above temperatures of 800 °C.<sup>[79]</sup> In fact, the only property silk lacks for use in electronic yarns is intrinsic electrical conductivity.

Thus far, literature has examined additives to silk allowing conductive silk composite fibers to be woven into textiles. A recent study by Nat et al. used heat and microwave radiation to make pyroprotein-based electronic yarns derived from com-

mercial silks.<sup>[79]</sup> Through a process of heating to 650 °C and microwave irradiation, commercial silk textiles were converted to electrically conductive pyroproteins without the need for extremely high temperatures or harsh chemical treatments.<sup>[79]</sup> Effectively, by inducing conductivity in silk fibers, Nat et al. has designed a method to remove one of the few demerits of silk as a hybrid material for electronic devices.

Taken together, through the addition of conductive fillers, pre- or post-treatment and through the pyrolysis of silk, silk-based electronic textiles have been made available. Still, there is plenty of room for improvement. In all of the examples above, *B. mori* silkworm silk was used as a starting material. This makes sense of course, as most silk-textiles are made of silkworm silk, but there are other alternatives that are ripe for study as well. Spider silk fibers offer many benefits including higher tensile strength and young's modulus compared to silkworm silk and may offer a viable alternative for woven conductive fibers.<sup>[18,80]</sup> Recombinantly produced silk proteins also offer potential functionality and tunability. These tailorable protein sequences could add specific binding motifs,<sup>[52]</sup> or add antibacterial properties<sup>[81]</sup> to name a couple of examples. Regardless of which direction electronic textiles develop in the future, silk will play a role in its development.

### 3.3. Sensors Made of Silk-Based Materials

Devices for recording biomedical signals such as in electrocardiography (ECG), electroencephalography (EEG), and to

collect evoked potentials data, are made of materials which are expected to be soft, hydrophilic, and electroconductive and are designed to minimize the stress imposed on living tissue during monitoring.<sup>[82]</sup> Silk is an ideal candidate to fulfill these requirements and offers many advantages including biocompatibility, biodegradability, and low cellular toxicity over traditional materials for use in medical applications.

Similar to work presented in the previous subsection, the first silk-based biological sensors involved a conductive polymer dope, specifically PEDOT:PSS.<sup>[82]</sup> Tsukada et al. successfully developed conductive silkworm silk-PEDOT:PSS threads. The initial conductivity was low ( $0.00117 \text{ Scm}^{-1}$ ) but the addition of glycerol increased the conductivity by two orders of magnitude ( $0.102 \text{ Scm}^{-1}$ ). Additionally, the silk-glycerol-PEDOT:PSS fibers showed improved durability and wettability of the composite threads allowing for repeated washing cycles while still retaining conductivity.<sup>[82]</sup> The threads were also successfully used for in situ ECG and EEG readings in rats providing not only a seminal first study with silk-based biological sensors but demonstrated practical use.<sup>[82]</sup>

Work by Zhang took a similar approach, using conductive graphene embedded into electrospun regenerated silk fibroin mats. The *B. mori* silk mats acted as a scaffold that trapped the graphene in the matrix. The trapped graphene could then act as a conductive material, while the scaffold retained the biocompatibility and mechanical properties of the silk matrix.<sup>[83]</sup> Similarly, Reizabal et al. used carbon nanotubes (CNTs) as their conductive material. The CNTs were dissolved with *B. mori* silk fibers in formic acid and then solvent cast to make thin films. The CNT fillers were found to be well dispersed in the polymer matrix and exhibited electrical conductivity and electromechanical responses. Interestingly, the authors found that the mechanical and thermal properties were independent of the quantity of CNT filler present in the silk matrix but the CNT did reduce  $\beta$ -sheet formation, and the electrical properties of the composite strongly correlated with the amount of CNT filler. Unique to this study, the CNT-silk composite films also exhibited a piezoresistive behavior opening a potentially promising new way to produce biocompatible stress sensors.<sup>[84]</sup>

Another particularly promising as well as surprising application for silk hybrid materials with conductivity are for sutures.<sup>[85]</sup> A recent study by Liu et al. produced biomimetic antibacterial opto-electro sensing sutures made from regenerated *B. mori* proteins. The core of the fibrous sutures was produced using wet spun using silk proteins dissolved in 99.5% 1,1,1,3,3,3-hexafluoro-2-propanol (HFIP). Silk fibers were then coated with silk-SWCNT, silk-GMCST (granulocyte macrophage colony stimulating factor), which is clinically used to improve cell growth and healing, and silk-GQD (graphene quantum dots) which simultaneously improves conductivity, increases antibacterial activity and allows for optical monitoring (Figure 4a). The resulting core-shell silk fiber was then tested in both cell and animal studies (Figure 4b–h). The results from cell studies indicated a strong antibacterial effect to *S. aureus* and *E. coli* when the suture was treated with small quantities of  $\text{H}_2\text{O}_2$  (Figure 4b). In addition, the GQDs were released to simulated body fluid indicating the potential of the fiber to act as a depot for delivery. (Figure 4c) Similarly, in vivo experiments with rabbits demonstrated that the silk sutures enhanced wound

healing, prevented growth of harmful bacteria, and through resistance testing the suture acted as a strain sensor for monitoring wound stress (Figure 4d–f).<sup>[81]</sup> The versatility exhibited by the silk suture hybrid materials is one of the many reasons why silk will play a pivotal role in shaping the future of renewable hybrid electronic devices.

## 4. Silk Composites and Hybrid Materials for Energy Conversion

As was shown in the previous section, silks can be incorporated as components in flexible electronic devices. Unsurprisingly, there is a wealth of new research showing that silk has the potential to produce the energy needed for said devices by means of conversion. Explored in this section are silk-based systems that show the potential of converting mechanical, thermal, chemical, and solar energy into electrical energy, as well as the role silk materials play in energy storage devices.

### 4.1. Mechanical Energy Conversion

Mechanical energy from the motion of wind and water has already been harnessed for human use for millennia to propel ships, windmills, and watermills. Following the industrial revolution, generators were coupled to wind- or water-driven turbines to convert the kinetic energy to electrical energy. Hydroelectric dams and windmill farms have since contributed significant amounts of energy in the global energy mix.<sup>[86]</sup> While these major sources of mechanical energy have been tapped extensively, other forms of exploitable mechanical energy have received less attention.

#### 4.1.1. Silk as a Material in Triboelectric Generators

People in modern societies regularly wear biopolymer-based clothing, and friction between the skin and clothing or between clothing and the surroundings inevitably occurs, especially in dry conditions. If two dissimilar materials come into contact with each other, the material with a higher surface electron affinity will attract electrons to its surface, resulting in it being negatively charged and leaving the other material positively charged. The basis of this phenomenon is called the triboelectric effect.<sup>[87]</sup> Rubbing two sufficiently triboelectrically-dissimilar materials together can potentially create a high enough voltage to power electrical devices.

This was demonstrated by Fan et al. in a seminal work.<sup>[88]</sup> In their study, they constructed a triboelectric nanogenerator by taping together a  $4.5 \text{ cm} \times 1.2 \text{ cm}$  rectangular PET ( $220 \mu\text{m}$ ) film and a Kapton ( $125 \mu\text{m}$  thick) film on the  $1.2 \text{ cm}$  edges. The upper and bottom parts were then sputter-coated with  $100 \text{ nm}$  of gold which served as electrode layers. Bending the films caused a rubbing together of the inner surface, which led to charge separation. They measured an output voltage of up to  $3.3 \text{ V}$  at a power density of  $\approx 10.4 \text{ mWcm}^{-3}$  (other works typically report power density using the unit  $\text{Wm}^{-2}$ ), which was enough to light up an LED. The nanogenerator was also used to charge

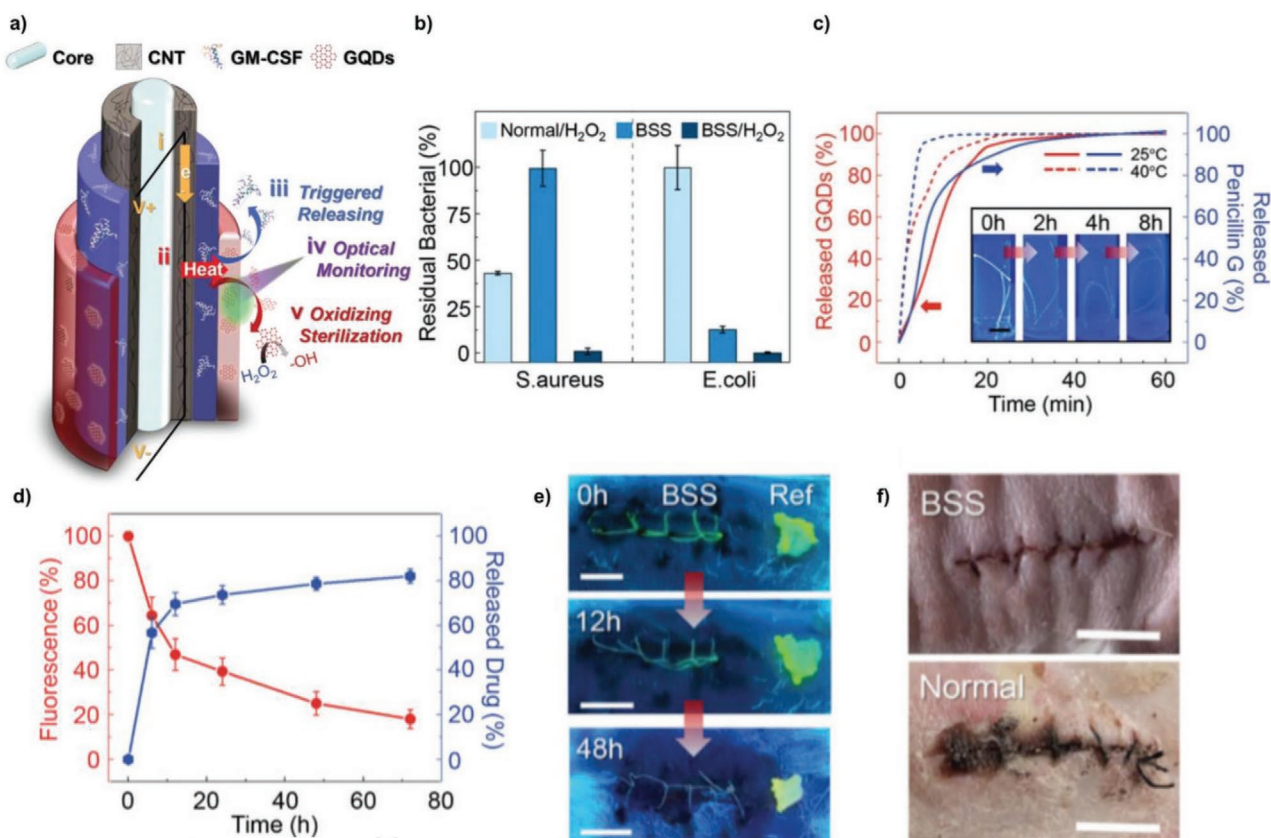


**Figure 4.** a) Schematic of the layered composition of the silk hybrid suture. The core consists of wet spun silk with outer layers of carbon nanotubes (CNT), silk treated with granulocyte macrophage colony stimulating factor (GM-CSF), and finally silk treated with graphite quantum dots (GQDs). b) In vitro characterization of the broad-spectrum antibacterial capability against *S. aureus* and *E. coli* on the normal suture with H<sub>2</sub>O<sub>2</sub>, the silk hybrid suture with (BSS/ H<sub>2</sub>O<sub>2</sub>) and without H<sub>2</sub>O<sub>2</sub> (BSS). c) Percentage of both released GQDs (red line) and released attached drug, Penicillin G, (blue line) of silk hybrid suture immersed in simulated body fluid with protease. Inset are photos of silk hybrid suture with GQDs replaced with Penicillin G under 325 nm UV light after 0, 2, 4, and 8 h. Penicillin G was used instead of GM-CSF to facilitate quantitative spectroscopy measurements in protease solutions. Scale bar: 0.5 cm. d) Fluorescence intensity (red line) and GM-CSF release degree (blue line) in percentages of silk hybrid suture, stitched on mouse's back wound under 325 nm UV light. e) Silk hybrid suture (labeled as BSS) images under UV light at 325 nm over 0, 12, and 48 h. The reference silk GQD composite was only placed around the wound during fluorescence measurements to be used as a reference initial intensity calibration. Scale bar: 0.5 cm. f) Photograph of the rabbit back wound stitched with silk hybrid suture (BSS, top) and normal sutures (bottom) after 11 days. Scale bar: 0.5 cm. Adapted with permission.<sup>[81]</sup> Copyright 2020, Wiley.

10 capacitors (22  $\mu$ F), charging them to 0.2 V in 450 deformation cycles. The durability of the nanogenerator was demonstrated by the steady voltage output even after  $\approx 10^5$  cycles of deformation (spanning about 30 days). This work is highly relevant because it demonstrated that such a simple, polymer-based nanogenerator could power a commercially available device. It also defined many of the routines such as the measurement of voltage and maximum power density, capacitor charging, and long-term deformation test as we will see in some of the works that we will describe below.

Silk is also a material that is suitable for constructing a triboelectric nanogenerator because it exhibits a strong triboelectric behavior, being placed only below wool in terms of the ease of electron loss in the triboelectric series.<sup>[89]</sup> Incorporating silk's intrinsic triboelectric property, Kim et al. investigated the effect of surface area morphology on the amount of voltage generated between the two contacting surfaces.<sup>[90]</sup> They used a setup, illustrated in **Figure 5**, which is similar to the setup described earlier by Fan et al with only minor changes. One half of the

triboelectric nanogenerator was created by attaching either an electrospun nonwoven mesh or a cast film of *B. mori* silk to an aluminum foil. The other half was created using attaching a polyimide film to an aluminum foil. The nanogenerator prepared with an electrospun nonwoven mat observed a peak voltage of about 16 V, about 1.5 times higher than the nanogenerator that used a cast silk film. Like Fan et al.'s device, the silk-based nanogenerator was able to light LEDs, and when loaded with a resistance of 5 M $\Omega$ , a peak power density of 4.3 mWm<sup>-2</sup> was measured. The nanogenerator was able to charge a 10  $\mu$ F capacitor to 2 V within 5 min, and also showed good durability, delivering steady voltage over 25 000 deformation cycles. This work is one of the earliest demonstrations of the possibility of incorporating silk into a triboelectric nanogenerator and achieving functioning performance by lighting up LEDs.

In a similar way a subsequent study by Liu et al.<sup>[91]</sup> explored the possibility of mass-producing silk film-based triboelectric generators by use of spray coating to replace the less scalable electrospinning used previously by Kim et al. In the study,



### Electric energy generation process

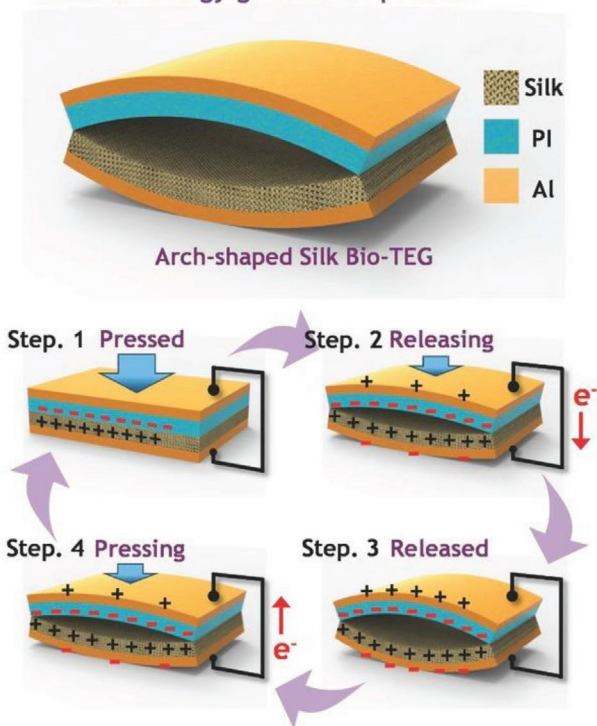


**Figure 5.** Schematics of the working principles of a silk-based triboelectric generator by Kim et al.<sup>[90]</sup> Step 1: By pressing the different electro-affine layers together, electrons can be transferred to the more electro-affine side. Step 2: Upon releasing the pressure, electrons begin to flow through the circuit to the oppositely charged side. Step 3: Upon full release, an electric field is created between the two sides as a result of the opposite charge difference on either side. Step 4: Reapplying pressure causes the electrons to flow in the reverse direction. Once the two sides are reconnected (Step 1), the process can be repeated. Reproduced with permission.<sup>[90]</sup> Copyright 2016, Wiley.

15 wt% aqueous silk solutions were spray coated between 5–15 s on 30 cm × 36 cm PET-ITO films. The nanogenerators showed V up to 218 V, and at a load resistance of 55 MΩ showed a peak power density of 68 Wm<sup>-2</sup>. The triboelectric generators also showed high durability, delivering consistent output voltage after 7 days with 300 cycles per minute.

These works have shown the potential of silk's triboelectric property in generating sufficient electricity to power existing electronic devices. From a seminal work that did not involve silk, a slight adjustment in the setup allowed the incorporation of silk in a triboelectric nanogenerator owing to silk's high processability. From that point on, the silk-based system could be optimized to show massive performance improvements and even upscaled for potential mass production.

#### 4.1.2. Silk as a Material in Piezoelectric Generators

Piezoelectricity is the generation of electrical potential difference due to the displacement of atoms in crystals with asymmetries in their lattice structure.<sup>[92]</sup> As silk is a semicrystalline material based on β-sheets, it is potentially capable of

piezoelectricity, which was demonstrated early on in 1939 by Harvey<sup>[93]</sup> who documented luminescence of silk when struck by a metal ball in a glass tube filled with neon gas. It wasn't until the 2010s that significant work examining the use of silk-based piezoelectric materials was conducted.

One recent example is a 2018 work of Karan et al.<sup>[10]</sup> They quantified the structure-dependent piezoelectric response of silk from the spider species *Nephila pilipes*, measuring out-of-plane piezoelectric coefficients up to ≈0.36 pmV<sup>-1</sup>. They then constructed a piezoelectric nanogenerator by embedding silk fibers, oriented in one direction, in a PDMS film and sandwiching the composite film between two electrodes, which could be connected to electronic devices. The nanogenerator was then subjected to various loads and deformation such as tapping with a finger, impact with a falling metal block, stretching, and twisting. The maximum output voltage, current, and power density were measured at ≈21.3 V, ≈0.68 μA, and ≈3.23 μWcm<sup>-2</sup> respectively. The voltage in particular proved superior compared to several other piezoelectric nanogenerators based on fish scale,<sup>[94]</sup> fish bladder,<sup>[95]</sup> and viral protein.<sup>[96]</sup> Similarly to the works described in the triboelectric section, the nanogenerator could power LEDs. Additionally, the nanogenerator could also power calculators, mobile screens, speakers, and wrist watches. They further examined the nanogenerator's potential of acting as a biosensor which requires high sensitivity to detect minute movements. To demonstrate this, they wrapped the nanogenerator around the experimenter's wrist and throat. The nanogenerator was able to detect arterial pulses and also generated distinct signals in terms of pattern and voltage for speech, swallowing, coughing, and gargling. To test the device stability, they activated the device using 1550 cycles of manual tapping and 30 000 cycles of sewing machine vibration, measuring in both cases a steady output voltage.

A more recent work by Huang et al.<sup>[97]</sup> also explored the possibility of energy conversion using a silk-based nanogenerator, but here combining both the piezo- and triboelectric phenomena. The nanogenerator used had a similar design to the one described in Figure 5. One half of the generator consisted of a poly(vinylidene fluoride) (PVDF) spin-coated onto a PET substrate. The other half consisted of a recombinant MaSp1 silk inkjet-printed onto a PET/ITO substrate. They tested the performance of a generator with a contact area of 6.25 cm<sup>2</sup> under a load resistance ranging between 1 and 100 MΩ. The nanogenerator showed peak performance with a loading of 8 MΩ, with a corresponding voltage, current, and power density of ≈200 V, 12 μA, and 4016 mWm<sup>-2</sup>. This power density was higher compared to other nanogenerators based on other materials, notably PVDF+paper,<sup>[98]</sup> PVDF+silk,<sup>[99]</sup> and porous PDMS,<sup>[100]</sup> which showed power densities of 3700, 3100, and 2330, respectively. For testing the long-term stability of the device, they performed 18 000 deformation cycles and recorded no significant change in the output current. The authors additionally conducted experimental controls using nanogenerators based either purely on PVDF/PET or silk/PET, which showed a voltage of 6 and 95 V respectively when connected to a load resistance of 10 MΩ. They argued that the much higher voltage (200 V) recorded in a piezo-triboelectric system cannot be explained by the simple addition of the voltages produced by the purely piezoelectric and purely triboelectric system, therefore the two

phenomena must have overlapped in a synergistic way. Moreover, the authors also conducted an in-vivo experiment, using a smaller version of the nanogenerator to monitor the heartbeat of rats. It has to be noted that in this work, PVDF is the source of the piezoelectricity, however as has been shown by Karan et al.,<sup>[10]</sup> oriented silk fibers can act as a piezoelectric material.

The tribo- and piezoelectric effects observed in silk-based nanogenerators are revealing the astounding potential of silk as a mechanical energy converter. These two effects observed in silk-based devices are sufficiently strong to power small devices, all with the help of an energy input normally regarded as negligible. They show high durability and simplicity in design, as well as the potential of being self-powered when combined with a capacitor. With further optimization, future small electronic devices may well run solely on silk-based nanogenerators.

#### 4.1.3. Silk as a Material in Osmotic Energy Devices

Osmosis describes the tendency of solvents to equalize concentration gradients of a solute across a semipermeable membrane. However, by limiting the movement of water and instead promoting the passage of ions through the membrane, a current can be generated across the membrane due to the net movement of charges. This is the basic principle of reverse electrodialysis, which has the potential to generate large amounts of energy, if there are systems in which two great bodies of liquid with a salt concentration gradient meet. Such systems occur quite commonly in nature. Estuaries, where river water meets seawater, can be found in all countries with rivers that flow into the ocean, giving great potential for use around the world.

Membranes with nanofluidic channels (channel diameter  $\leq 100$  nm) are suitable for generating electricity from solute concentration gradients. The surface charge of the channels acts as a filter, repelling ions with like charges and allowing the passage of ions with opposite charges through the channels.<sup>[101]</sup> Silk is an ideal material for such membranes because of its tunable surface charge<sup>[47,48]</sup> and processability into membranes.

Xin et al.<sup>[102]</sup> used *B. mori* silk fibroin as a component in a bicomponent membrane for osmotic energy conversion. The membrane was produced by filtering a 0.05 wt% aqueous silk solution through an anodic aluminum oxide (AAO) membrane (pore size between 80–100 nm, 60  $\mu\text{m}$  thick), thereby creating a porous layer of deposited silk fibroin (pore size  $\approx 20$  nm, 5  $\mu\text{m}$  thick). The deposited layer showed neither dissolution nor delamination from the AAO membrane after having been soaked in deionized water for 93 days. This stability was attributed to the strong hydrogen bonds formed between fibroin/fibroin and fibroin/AAO membrane. For testing its performance, the membrane was placed in a slot in the wall that separated the two compartments of an electrochemical cell. One compartment contained a 0.01 M NaCl solution while the other a 0.5 M NaCl solution, whereby the 50-fold concentration gradient corresponds to that between river- and seawater. When connected to an external load of about 23 k $\Omega$ , the observed peak power density was  $\approx 2.86$  Wm<sup>-2</sup>, which indicates that silk can be used for osmotic energy conversion.

Chen et al.<sup>[103]</sup> conducted a similar study a year later, using only *B. mori* silk to produce an ultrathin, single-component membrane by spin coating. Each spin coating cycle produced single silk film layers of 10 nm, thus a membrane of variable thickness could be created by repeatedly casting subsequent layers on top of the preceding ones. The membranes were 3% porous with pores of sizes about 75 nm. They were robust enough for handling and were insensitive to changes in the pH of the electrolyte, which was varied in between 3 and 11. Not only did the membranes remain intact, the current across the membranes did not vary significantly with pH, showing the wide range of pH in which the membranes can operate while still delivering a steady current. In testing the performance of the membrane, they used a 50-fold salinity gradient and measured a power density of 4.06 Wm<sup>-2</sup>, which not only surpassed that of Xin et al., but of an MXene/Kevlar membrane reported by another group a year earlier<sup>[104]</sup> which they claimed to be the state of the art.

These studies showed the potential of silk and silk-based membranes in osmotic energy conversion. Silk is easily processed into membranes with nanofluidic pores, whose charge and thickness can be tuned. These membranes demonstrated long-term stability in water and are insensitive to pH changes in terms of integrity and performance. They also deliver power densities on par with comparable materials.

#### 4.2. Thermal and Thermoelectric Energy Conversion

Heat is usually an undesired byproduct of processes such as exothermic chemical reactions, Ohmic heating of electrical components, and friction between mechanical parts. Typically, heat is treated as a waste produce to be removed. However, in doing so, a significant amount of energy is wasted during the removal process and more recently, efforts to reduce energy consumption and increase process efficiency have led to heat recovery measures being implemented.<sup>[105]</sup> This includes using the otherwise wasted energy from various processes to, for example, pre-heat materials in pre-processing, heating/cooling ambient air in buildings, and heating tap water for toilets and showers to name a few.<sup>[106]</sup>

The potential heat-related applications of silk are being discovered by two separate veins of research. The first seeks to understand the biological role that silk plays in the development of arthropod pupae and embryos. Here research is beginning to reveal that silk forms more than a passive, isolating shell that protects developing arthropods from predators<sup>[107]</sup> and extreme weather conditions.<sup>[108]</sup> Even prior to any human intervention, silk possesses remarkable thermoregulatory properties. A 1995 study by Ishay et al. examined the electrical response of the silken nest caps towards changes in the heat. Sealed wasp nests of the species *Vespa orientalis* that contain pupae exhibit the ability to maintain a temperature between 28–30 °C even in the absence of adults that usually aid in thermoregulation. To investigate the role of the silk nest caps in thermoregulation, the authors collected the nest caps and subjected them to differing temperatures while measuring the current generated across the caps, revealing a dependence between current and temperature with a peak current of several hundred nanoamperes measured between 28–31 °C. In discussing the observation, the authors postulated that this indicates the electric charge storage capability of silk.<sup>[109]</sup>

In the context of pupae, the generated current might be sufficient as a backup heating mechanism in the event that adult wasps are absent for extended periods of time. However, the generated nanoampere current is barely useful for any human application. A later work in 2014 by Tulachan et al.,<sup>[110]</sup> which was based on the earlier works of Ishay,<sup>[109,111,112]</sup> showed in a clearer demonstration the potential of natural silk cocoons in human application. In the initial setup of their experiment, they used empty *B. mori* cocoons and attached aluminum foil inside the cocoons as an electrode. They then spooled copper wire around the outer surface of the cocoons, which served as the counter electrode. Three of the cocoons were then connected in series with a red LED that required a minimum voltage and current of 1.6 V and 18  $\mu\text{A}$ , respectively. Upon exposing the cocoons to hot water vapor, the LED lit up, demonstrating that silk cocoons in their natural form can already function as a sort of moisture-triggered battery.

For making standardized devices, they replaced whole cocoons with smaller units made of rectangular, 2.5 cm  $\times$  1 cm sections of the cocoons. Each device consisted of four units connected in series. These were used in further testing, including measuring voltage and current as a function of time. When the devices were exposed to water vapor, they measured steady values for voltage ( $\approx 0.5$  V) and current ( $\approx 1$   $\mu\text{A}$ ) for up to 200 min, at which point both values started to drop. This drop however was shown to be reversible. After letting them dry for 1 h, they were exposed again to water vapor, which again showed steady voltage and current reading for another 200 min. These works revealed the remarkable untapped potential of naturally occurring cocoons in powering small electronics.

The second vein of research examines silk's potential in composites, with silk playing a role as a template for thermally active species. Anticipating the widespread use of silk-based electric devices in the future, Tsao et al. 2015 examined the phenomenon of white-light-induced heating in *B. mori* silk films embedded with Au nanoparticles. Composite films were prepared by a facile method of casting a mixture of silk solution and Au nanoparticles (of various sizes and at various Au-to-silk weight ratios) onto a fused silica plate or a Si device measuring 1.5 cm  $\times$  1.5 cm, with the optimal composite film containing 25 wt% Au, and the Au nanoparticles being 13 $\pm$ 2 nm in size. When subjected to multiple 5 min cycles of exposure to white LED light of 200 mW cm<sup>-2</sup> followed by 5 min of non-exposure, the film showed rapid heating up to 100  $^{\circ}\text{C}$  and cooling to room temperature without any reduction in performance.<sup>[11]</sup>

Using a different silk morphology, Zhang et al.<sup>[113]</sup> examined the potential of silk cloth as a substrate for reduced graphene oxide in steam generation applications, citing silk's mechanical properties, thermal stability, permeability in air, and hygroscopicity as the motivation of using silk as a material. They dyed the silk cloth with graphene oxide, which was subsequently reduced by microwaving at 95  $^{\circ}\text{C}$  for 10 min with 300 W power input. The dyed silk cloth was used to cover the upper surface of a polyethylene foam that floats on top of a water surface, with the outer parts of the silk cloth dipping into the water. The capillary effect of the cloth ensures that water is continuously wicked towards the upper surface of the foam while water evaporates at the top due to heating. This setup exhibited high efficiency, generating steam at 1.48 kg m<sup>-2</sup> h<sup>-1</sup> under one solar irradiance (power per unit area of electromagnetic radiation received from the sun for

a specific wavelength range) after 30 min of exposure, which is about 5.7 times more efficient compared to water evaporating on its own under the same irradiance. In addition, the dyed silk fabrics were stable and able to withstand up to 30 washing cycles without any significant loss in conversion efficiency. Such a simple system may be upscaled for practical applications such as large-scale water sterilization and desalination.

These studies point out that silk has a great potential for application in thermal energy conversion. Naturally occurring *V. orientalis* nest silk caps and *B. mori* cocoons showed an interesting electrical response to heat and humidity, which in the latter case was even sufficient to power an LED. For composites, silk can be easily processed into flexible and durable templates which immobilize various thermally active species for thermal energy conversion devices.

### 4.3. Chemical Energy Conversion

Much of the modern world is built upon generation of energy from chemical reactions. From rocketry to combustion engines to batteries, chemical reactions, specifically the breaking of chemical bonds, are the main source of energy production in the world today.<sup>[114]</sup> This energy production comes at significant cost to the environment, and with ever more increasing demand for green energies to curb the rising threat of climate change, scientists have turned to nature for solutions. A more environmentally friendly approach to the increasing energy demand has seen a decrease in coal and oil use for energy production in the western world<sup>[115–118]</sup> but with energy consumption estimated to double by 2050, and with mounting pressure to move away from fossil fuels, renewable energy sources require ever more creative solutions to keep up with demand.<sup>[119–121]</sup>

Changing how energy is produced is one of many steps that must be undertaken to curb the environmental impact of mankind. New renewable, biocompatible, and degradable materials are also highly sought after with the ultimate goal to have a net neutral environmental impact.<sup>[118,120]</sup> One such energy source that is often studied in literature is the oxygen reduction reaction, which is the primary driving force for fuel cells.<sup>[122]</sup> While fuel cells can be built from a myriad of different reduction reactions to produce energy, the two main reasons as to why oxygen remains the preferred cathodic fuel are its abundance in the earth's atmosphere and the fact that its fully reduced form, water, is non-toxic. The main limitation to performance of fuel cells is the slow reaction kinetics of oxygen reduction. Platinum is commonly used as a cathode catalyst to speed up the reaction kinetics, but due to the expense and scarcity of platinum it limits widespread use in fuel cells.<sup>[12]</sup> Therefore, it is important to find an alternative catalyst that is readily available and cost effective.

#### 4.3.1. Oxygen Reduction Catalysis

Proteins and their subsequent nanostructures have become increasingly sought after for their promising materials design potential, in particular, to develop protein inspired structures to harness ion transport for bioelectric generation.<sup>[123–125]</sup> Of particular note, silk nanofibrils, derived from cocoons of

*B. mori* silkworms, can be produced with very high aspect ratios leading to high surface areas for potential use in oxygen reduction catalysis.<sup>[126]</sup> Given that silk nanofibrils are easy to produce, naturally abundant, and both biocompatible and biodegradable, it is no surprise that silk stands as one key material for use in green energy production.<sup>[127]</sup>

Zhou et al. used naturally collected spider silk samples produced by *Pholcus opilionoides* as the base material for carbon nanofiber scaffolds to be used as oxygen reducing catalysts.<sup>[128]</sup> While not directly using spider silk for scaffolds but its carbonized imprint, this seminal work demonstrates that spider silk materials could be converted into usable materials through a facile method of heating and acid treatment. Furthermore, the resulting scaffolds exhibited high catalytic activity for oxygen reduction, which the authors attribute to the large number of activation sites present on the scaffold.<sup>[128]</sup> Interestingly, the large surface area found on the carbon nanofiber scaffolds was attributed to small mesopores that formed on the surface during silk to carbon nanofiber conversion. Thus, this methodology of carbonization may be used for increasing or tuning the surface area of other carbonized silk fibers and carbon nanofibers.<sup>[128]</sup>

In a similar study, Rapson et al., used a hybrid heme-honeybee silk protein recombinantly produced using *E. coli* to generate films useful for oxygen reduction materials.<sup>[12]</sup> Rapson et al. had previously designed a process to immobilize the active heme porphyrin ring of myoglobin onto the silk backbone via direct coordination of a histidine residue.<sup>[129,130]</sup> This process was also performed with recombinant honeybee silk, and the gained hybrid material was then processed into films. These films were shown to efficiently reduce oxygen functioning as an electrocatalyst. Additionally, the heme-silk films produced negligible amounts of hydrogen peroxide, a side reaction that can occur during the reduction of oxygen using metallic catalysts which causes corrosion and eventual failure of the cathodes. Not only did the introduction of the heme-silk films increase stability of the fuel cells tested, the heme-silk films were capable of reducing oxygen efficiently in neutral buffers, which opens opportunities for design of enzymatic or microbial fuel cells.<sup>[12]</sup>

#### 4.4. Energy Storage Using Silk-Based Materials

In addition to developing new renewable materials for solar and alternative energy devices, there is an increasing demand for energy storage devices with high energy density, long life times, and low material costs.<sup>[131]</sup> Currently, battery and capacitors are dominated by alkali metals, specifically Lithium. The demand for lithium, primarily used in lithium-ion batteries, has more than tripled between 2015 and 2020 and is expected to grow by more than 500% to reach 2.2 million tons by 2030.<sup>[132,133]</sup> This increase will only add to the growing mineral crisis as the world moves to more environmentally friendly technologies.

##### 4.4.1. Carbonized Silk for Batteries and Super Capacitors

More renewable and recyclable materials are already being developed for use in the battery market to combat the looming mineral crisis. In particular, a recent study by Wu et al. used

a nanofiber film of regenerated silk, harvested from *B. mori* cocoons, as an interlayer of Li–S batteries.<sup>[134]</sup> The silk fibroins were electrospun and carbonized and sandwiched as a double layer between the S-cathode and Li-anode (Figure 6).<sup>[134]</sup> The carbonized silk fibers (SCNFs) were successfully woven into a continuous conductive network, which provided fast electron pathways and acted as a cathode and anode interlayer delivering a high discharge capacity and remaining stable for 200 cycles.<sup>[134]</sup> The enhancement effect seen by the interlayers greatly increased the coulombic efficiency and charge retention life of the battery, opening potentials for significantly increasing Li–S battery stability.

Similarly, an earlier study by Hou et al. demonstrated that porous nitrogen-doped carbon nanosheets derived from *B. mori* silk can be produced for high capacity battery anodes and supercapacitors. The silk was treated with metal salts, FeCl<sub>3</sub> and ZnCl<sub>2</sub>, which were not only effective at dissolution and regeneration of natural silk, but the metal salts could simultaneously act as activation sites for carbonization agents.<sup>[135]</sup> The resulting nanosheets assembled in lamellar-like layered structures as is expected from silk materials. Unique to this system, the lamellar-layered structures contained both micro- and mesopores giving them an extremely high surface area. This lamellar-layered structures showed a high storage capacity of 1865 mA h g<sup>-1</sup> and only a 9% stability loss after 10 000 cycles (traditional rechargeable batteries show complete stability loss at around 10 000 cycles) thus paving the way for organic silk-based batteries for potential commercial use.<sup>[135]</sup>

Carbonization of natural silk for anode/cathode interlayers is not the only useful route towards applications. Integration of flexibility, biocompatibility, and degradability for energy storage/delivery devices for epidermal and implantable bioelectronics are a particular topic that Pal et al. has recently explored. The authors demonstrated that *B. mori* silk in conjunction with conducting polymers, such as poly(3,4-ethylenedioxythiophene), polystyrene sulfonate, or graphene could be used

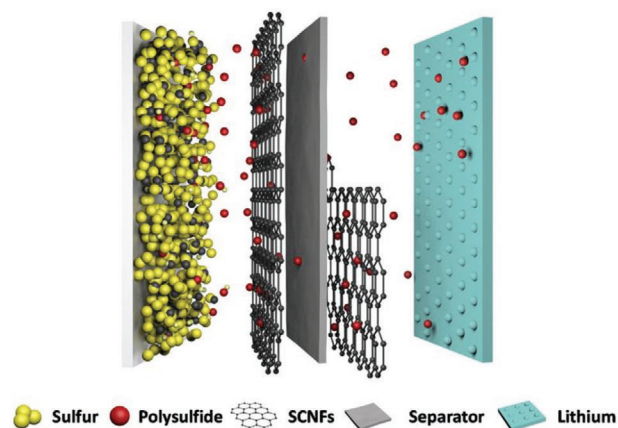


**Figure 6.** Schematic of assembled Li–S cell featuring sulfur cathode, cathode interlayer, separator, anode interlayer, and lithium metal. Smaller impedance was achieved for the cathode interlayer (left half) but at cost of polysulfides damaging the Li-metal after long cycling times. Addition of the carbonized silk layers in between the cathode (left half) and anode (right half) not only provided fast electron transport but also captured polysulfides during charging, preventing corrosion of the Lithium interlayer. Reproduced with permission.<sup>[134]</sup> Copyright 2019, Elsevier.

in photo-patternable biocomposite inks. Uniquely, these inks could be fabricated into active electrodes and printed on flexible protein sheets using photolithography under benign conditions with only water as solvent, thus, eliminating many of the harsh metal ion solvents necessary in the aforementioned studies.<sup>[58]</sup> These patterned thin films showed high capacitance, power density, and cycling stability over 500 cycles. Furthermore, the thin films were shown to be cytocompatible and completely degraded over a period of 1 month which may indicate an application as biodegradable batteries.<sup>[58]</sup>

Unlike traditional lithium ion batteries, supercapacitors have much faster charge rates, can store more energy and have longer lifespans (100 000 to 1 000 000 million cycles compared to 500 to 10 000 of lithium ion batteries).<sup>[136]</sup> These benefits are offset by a slow self-discharge rate which causes the supercapacitor to be poorly suited for long term energy storage. In addition, supercapacitors suffer from gradual voltage loss, which causes the voltage output of capacitors to decline linearly with their stored charge (lithium ion batteries have near-constant voltage output regardless of charge). Still due to the wide range of operating temperatures, supercapacitors have seen use in hybrid vehicles, use in conjunctions with batteries for hybrid or quick charging energy storage devices, and as backup systems and power buffers.<sup>[136,137]</sup> It should come then as no surprise that supercapacitors have become a promising field of study for silk-based power sources and energy storage devices.

One early work examined the preparation of nitrogen enriched carbon materials from *B. mori* silk fibers.<sup>[138]</sup> Using heat treatment, the authors converted the silk fibroin to nitrogen-containing activated carbon, which they then successfully used for applications in electric double layers for supercapacitors.<sup>[138]</sup> Building upon this work, in a more recent study porous nitrogen-doped carbon-derived films were designed from *B. mori* silk for use in potassium-ion hybrid capacitors.<sup>[139]</sup> The resulting nitrogen rich, porous carbonized silk anode exhibited a power density of 112.6 W kg<sup>-1</sup>, and could be fully charged in just 7 min with a discharge time of 2.5 h.

#### 4.4.2. Silk-Graphene Self-Assembly for Energy Storage

Work discussed thus far in energy storage has focused on the conversion of silk to carbonized silk for use as anodes in batteries or super capacitors. While this certainly shows the flexibility and usefulness of silk from a materials perspective, silk also has many other properties that are useful for energy exploitation.

One such example is the natural ability of silk proteins to self-assemble. Wang et al. demonstrated that a mixture of graphene and *B. mori* silk fibroin dissolved in KOH yielded self-assembled structures that could then be freeze-dried to form aerogels, and through a carbonization process graphene-silk composite materials could be obtained.<sup>[140]</sup> The harvested graphene-silk nanofibril composite material exhibited remarkable electrochemical stability with a capacitance retention ratio of 96%.<sup>[140]</sup> In addition, the composite material achieved high energy density paving the way forward for use as a material for the manufacturing of supercapacitors with both high performance and low cost.

Building upon similar work, Yun et al. produced carbon aerogels based on regenerated silk proteins and graphene oxide. The aerogels were prepared using a flash freezing/lyophilization process.<sup>[141]</sup> The hydrophilic blocks of the silk proteins showed strong interactions with the oxygen functional groups of graphene oxide resulting in silk-graphene composite nanoplates assembling into 3D cryogels during a lyophilization process. These cryogels could then be converted to aerogels via treatment using methanol. The resulting materials exhibited a high capacitance of 298 Fg<sup>-1</sup> and stability over 5000 repeated cycles.<sup>[141]</sup>

#### 4.5. Solar Energy Conversion

One of the more promising future directions is the use of recombinant spider silk for example as a fibrous scaffold for Au and TiO<sub>2</sub> nanoparticles for use in photocatalytic water splitting yielding hydrogen. In a paper by Herold et al. recombinant spider silk was successfully modified with respective binding motifs to selectively interact with Au and TiO<sub>2</sub> nanoparticles, designated ntag<sup>Cys</sup>eADF4(κ16) and eADF4(C16)-TiO<sub>2</sub>-bp, respectively.<sup>[52]</sup> Using a facile technique of film casting and capillary force-based patterning, the proteins were processed into patterned films with a base of Au-binding ntag<sup>Cys</sup>eADF4(κ16) and stripes of TiO<sub>2</sub>-binding eADF4(C16)-TiO<sub>2</sub>-bp (Figure 7). Upon particle immobilization, Au and TiO<sub>2</sub> nanoparticles were perfectly aligned along the stripes, and the interface in between was found to successfully be able to catalyze the photoinitiated splitting of water producing hydrogen under the exposure of light at the visible wavelength providing a basis for further development of recyclable hybrid materials for water splitting photocatalysis.<sup>[52]</sup>

The result of Herold et al. is of particular interest for several reasons. First, the specific binding of nanoparticles was accomplished through explicit genetic modification of the protein, that is, protein engineering. Thus, various nanoparticles can be attached upon sequence variation of the underlying spider silk protein, making a robust, tunable material for hybrid energy needs. Second, spider silk proteins can be processed into not only 2D structured films but also into fibers and fiber meshes. No processability problems arise after modification and binding. Lastly, the nanoparticles show specific binding to the specifically modified proteins allowing for patterning and a myriad of new possible spider silk-nanoparticle hybrid energy materials. Additionally, with the ability to recombinantly produce silk proteins with selective binding motifs, there is a vast potential for scalability.

The work by Ma et al. provides another very promising future direction for silk hybrid materials for solar energy conversion. Their work focuses on producing deformable, malleable silk-based perovskite solar cells using *B. mori* silk.<sup>[142]</sup> Combining silk fibroin and silver nanowires, the films were capable of deforming into a diverse range of structures from simple (bending, folding, and stretching) to complex origami (flower, bowknot, and paper crane) (Figure 8a). The malleable films could be deformed and subsequently recovered to their original shape through the exposure to water (Figure 8b,c). SEM images of the recovered films showed no signs of grain boundaries or crack formations and only minor

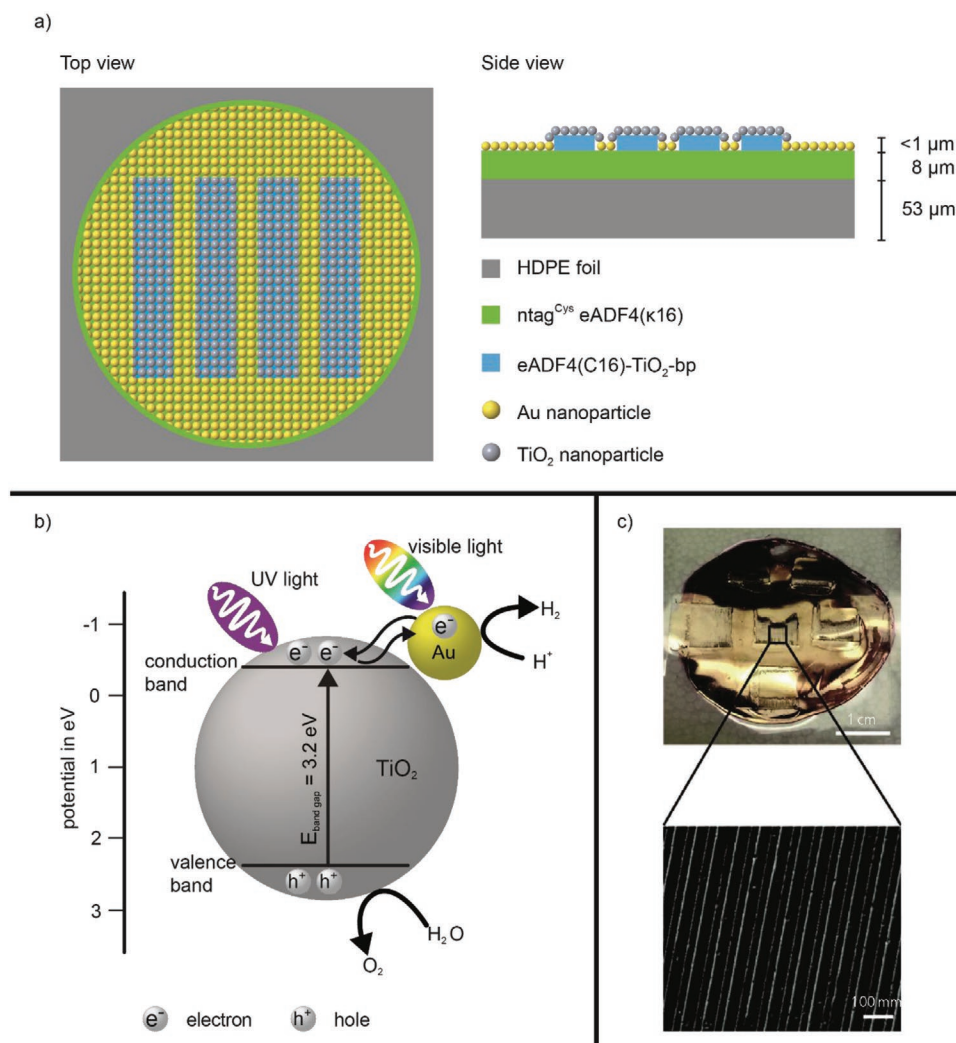


**Figure 7.** a) Schematic top and side view of a patterned film based on recombinant spider silk proteins for use in photocatalytic water splitting. The Au-binding ntag<sup>Cys</sup>eADF4(κ16) forms the base while the TiO<sub>2</sub>-binding eADF4(C16)-TiO<sub>2</sub>-bp forms stripes on the base layer. Au and TiO<sub>2</sub> nanoparticles bind selectively to the respective proteins, creating Au-TiO<sub>2</sub> interfaces at the edge of the stripes. b) Schematic of the photocatalytic water splitting reaction occurring when Au and TiO<sub>2</sub> are hybridized. c) Photograph of the patterned film after Au coupling and TiO<sub>2</sub> toning and a light microscopy image of the patterned Au doped silk film. (c) Adapted with permission.<sup>[52]</sup> Copyright 2018, ICE Publishing.

deformations in the films (Figure 8d,e). The films showed similar sheet resistances in the undeformed and deformed state, indicating no significant loss of electrical conductivity during deformation.<sup>[142]</sup> These sheets could then be employed in photovoltaic cells using layers of PEDOT:PSS, perovskite (CH<sub>3</sub>NH<sub>3</sub>PbI<sub>3</sub>), phenyl-C61-butyric acid methyl ester (PCBM), and Ag. These sandwiches were capable of simple bending and stretching without significant loss of function. In addition, the photovoltaic cell obtained a respectable power conversion efficiency of 10.4% and there was no decrease in efficiency after stretching the device 10 times (with strains of 50%) with the device showing little deterioration of the perovskite layer in SEM images.<sup>[142]</sup> However, when the device was stretched with 50 stretching cycles, the power conversion efficiency was reduced by up to 60% with the perovskite layer showing significant deterioration in SEM images.<sup>[142]</sup> Still, the work here marks an important seminal step in malleable, flexible silk-based solar energy research.

Much like the water splitting result, there are several promising results from the Ma paper. The most obvious result is the ability to make both, simple and complex shapes which may lead to unique ways to increase surface areas of future solar cells. While the solar device did lose efficiency after repeated stretching cycles, combining silk's flexibility with perovskite's excellent photoelectric and ferroelectric properties is something that should not be ignored. Deformable devices may still have a way to go, but the ability to make malleable perovskite solar devices using a biocompatible, environmentally friendly material like silk is supremely promising.<sup>[143–146]</sup>

## 5. Conclusions and Future Outlook

Considering the sheer number of diverse topics covered in this review one can begin to see the versatility of silk as a material.

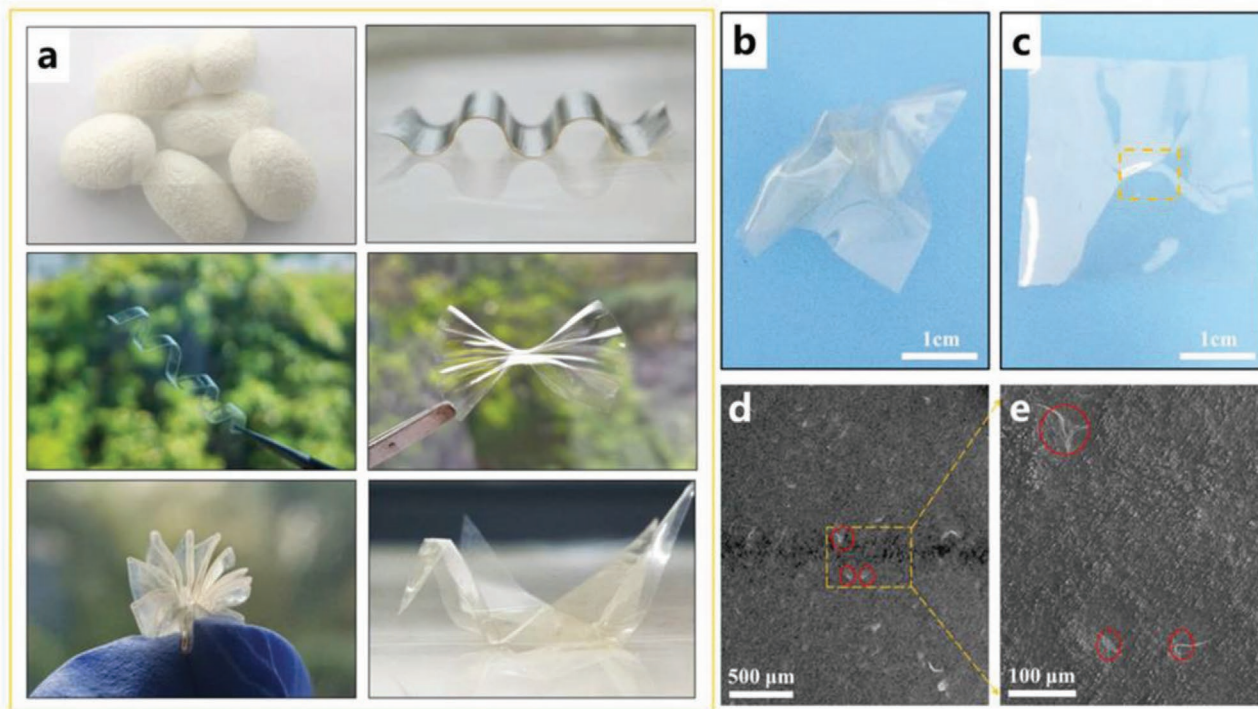


**Figure 8.** a) Photographs of silkworm cocoons and the silk-perovskite films showing the malleability and pliability of the films folded into different origami shapes. b) Photograph of silk-perovskite composite film to be used as a flexible solar energy device after random crumpling. c) Photograph of silk-perovskite after exposure to water vapor resulting in crumple recovery and reversible wrinkling. d) SEM image of recovered silk-perovskite film. e) Magnification of the crumpled region. Red circles denote localized wrinkle deformations but no cracks or grain boundaries are present. Reproduced with permission.<sup>[142]</sup> Copyright 2020, Wiley.

As a summary, **Figure 9** illustrates the multifunctionality and many applications for silk in protein-based hybrids for energy systems. From simple to complex materials, one only has to look at several examples from the above to see how silk will be used in the future. Carbonization of silk to replace fossil fuel derived conductive graphene,<sup>[135]</sup> biocompatible, thermally resistant, flexible fabrics,<sup>[58,63,79,147]</sup> scaffolds for biocatalytic reactions,<sup>[12,128]</sup> specific binding motifs for nanoparticle binding,<sup>[52]</sup> flexible triboelectric generators and photovoltaic devices,<sup>[90,91,142]</sup> and sutures that offer antibacterial activity, controlled drug release and active conductivity and monitoring<sup>[81]</sup> are but a few of the many examples of the future of silk based hybrid materials.

Still, silk-hybrid materials are not without their fair share of issues and there are some problems that must be overcome in the future if silk is to find common use in hybrid energy materials. First, mass production of silk is a major drawback at the moment. Harvesting, for example, spider silk is by far not as efficient as producing synthetic polymers or even harvesting polysaccharides such as cellulose. This has led to an increase in the production of recombinant silk proteins. Our problem is long term stability. Degradation is a problem that all organic materials face, and though silk is particularly resistant to thermal and environmental degradation compared to most polymers, biopolymers, and proteins, it still degrades in UV-light, undergoing photo-oxidation and eventual damage/loss of crystallinity.<sup>[148]</sup> Much like many other synthetic polymers that have similar issues, this limits silk's long term use

in many devices that are constantly exposed to light irradiation. Finally, silk is not conductive without pre- or post-treatment.<sup>[135]</sup> This often means conductive fillers are added to devices, which lack the mechanical properties of silk. The mismatch in mechanical properties can lead to breakage and degradation of the conductive layers or delamination of the silk, a problem that needs to be considered when making hybrid devices, as this often significantly affects device efficiency and function.

Despite some drawbacks, it's silk's flexibility and multifunctionality that will define its legacy moving forward. Consider that the versatility and multifunctionality of silk is not mutually exclusive to its application. No better example of this is the multifunctional uses of silk-based sutures that encompass both conductive fibers for wound stress monitoring, drug encapsulation and release, and antibacterial activity.<sup>[81]</sup> Any one of these properties would be beneficial in a material but there are few materials other than silk that could produce all three in a single fiber.

But the versatility and multifunctionality of silk goes deeper than just mixing and matching the different properties of silk desired for a specific application. Consider, that with a facile genetic modification to a silk protein, a specific binding motif can be inserted that selectively binds nanoparticles, completely changing the role silk plays in a solar conversion device.<sup>[52]</sup> There are few, if any, materials that could offer all of the benefits (i.e., mechanical strength, biocompatibility, renewability, etc.) of natural silk and still be tunable molecularly. And that tunability is the true value of silk as part of a

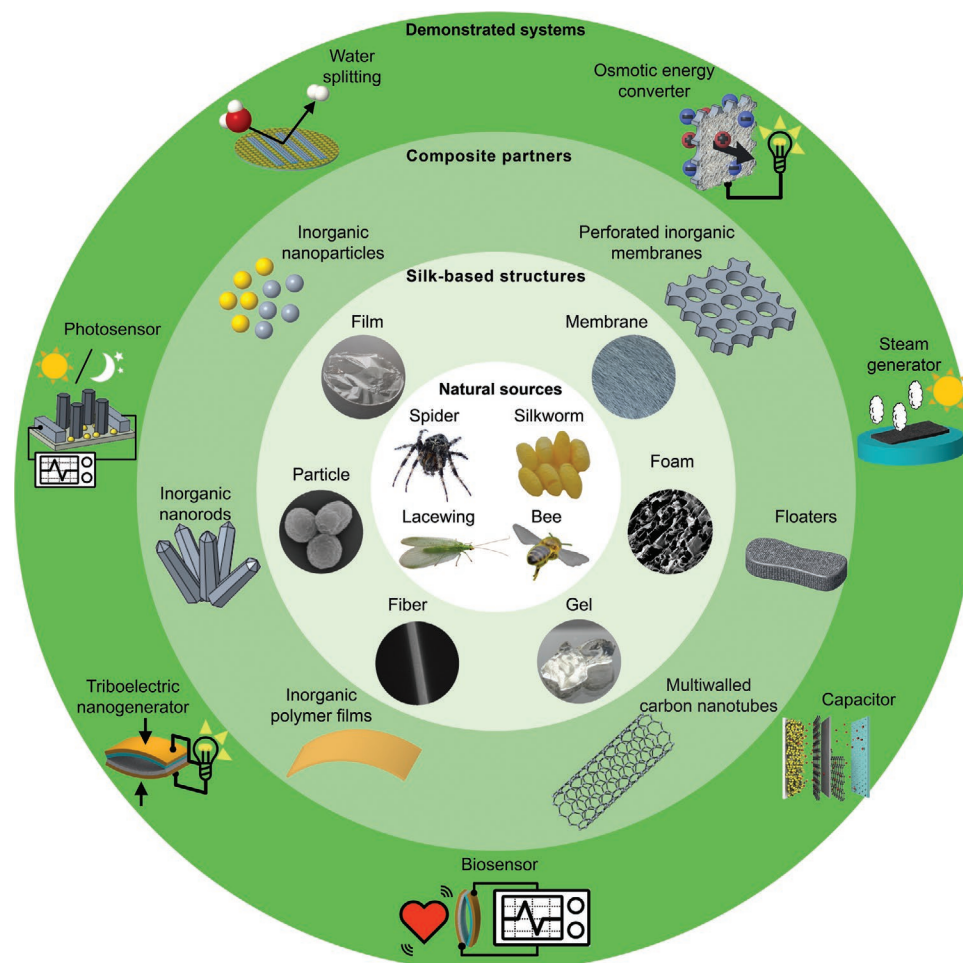


**Figure 9.** Silk proteins can be processed into various structures. These structures, once combined with other materials (e.g., inorganics, polymers, or carbon nanotubes) either as composites or hybrids, have demonstrated a wide range of energy conversion and storage potential. The triboelectric nanogenerator image is adapted with permission.<sup>[90]</sup> Copyright 2016, Wiley. The capacitor image is reproduced with permission.<sup>[134]</sup> Copyright 2019, Elsevier.

hybrid material. How many other polymers, polysaccharides, or proteins can offer so many material merits and then also the ability to fundamentally change their function with simple chemistry?

As a final thought, with energy consumption estimated to double by 2050,<sup>[119–121]</sup> there is a looming energy and climate crisis on the horizon. As demands for “greener” materials for alternative energy sources rise, silk-based materials have already shown versatility and tunability as the material of choice for many of the energy needs moving forward.

## Acknowledgements

The authors would like to thank Tim Schiller for helping in preparing the water splitting schematic in Figure 7.

Open access funding enabled and organized by Projekt DEAL.

## Conflict of Interest

The authors declare no conflict of interest.

## Keywords

energy conversion, energy storage, renewables, silk, silk hybrid, solar energy

Received: February 12, 2021

Revised: April 28, 2021

Published online: May 16, 2021

- [1] B. Petroleum, *BP Statistical Review of World Energy 2020*, London 2020, <https://www.bp.com/content/dam/bp/business-sites/en/global/corporate/pdfs/energy-economics/statistical-review/bp-stats-review-2020-full-report.pdf> (accessed: November 2020).
- [2] D. A. Lashof, D. R. Ahuja, *Nature* **1990**, 344, 529.
- [3] F. Johnsson, J. Kjärstad, J. Rootzén, *Clim. Policy* **2019**, 19, 258.
- [4] M. Kaneko, A. Yamada, in *Solar Energy-Phase Transfer Catalysis-Transport Processes*, Springer, New York **1984**, p. 1.
- [5] M. K. H. Rabaia, M. A. Abdelkareem, E. T. Sayed, K. Elsaid, K.-J. Chae, T. Wilberforce, A. G. Olabi, *Sci. Total Environ.* **2021**, 754, 141989.
- [6] C. Aguilar, J. Herrero, M. Polo, *Hydrol. Earth Syst. Sci.* **2010**, 14, 2479.
- [7] R. E. Blankenship, *Plant Physiol.* **2010**, 154, 434.

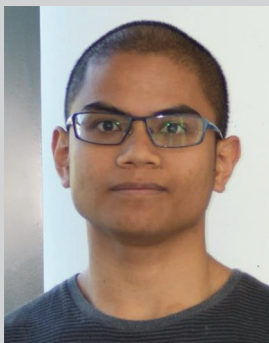


- [8] M. Becquerel, C. R. *Hebdomadae Seances Acad. Sci.* **1839**, 9, 561.
- [9] H. Spanggaard, F. C. Krebs, *Sol. Energy Mater. Sol. Cells* **2004**, 83, 125.
- [10] S. K. Karan, S. Maiti, O. Kwon, S. Paria, A. Maitra, S. K. Si, Y. Kim, J. K. Kim, B. B. Khatua, *Nano Energy* **2018**, 49, 655.
- [11] S. H. Tsao, D. Wan, Y.-S. Lai, H.-M. Chang, C.-C. Yu, K.-T. Lin, H.-L. Chen, *ACS Nano* **2015**, 9, 12045.
- [12] T. D. Rapsom, R. Kusuoka, J. Butcher, M. Musameh, C. J. Dunn, J. S. Church, A. C. Warden, C. F. Blanford, N. Nakamura, T. D. Sutherland, *J. Mater. Chem. A* **2017**, 5, 10236.
- [13] A. Goetzberger, C. Hebling, H.-W. Schock, *Mater. Sci. Eng., R* **2003**, 40, 1.
- [14] N. Abas, A. Kalair, N. Khan, *Futures* **2015**, 69, 31.
- [15] D. Klemm, B. Heublein, H.-P. Fink, A. Bohn, *Angew. Chem., Int. Ed.* **2005**, 44, 3358.
- [16] X. Wang, C. Yao, F. Wang, Z. Li, *Small* **2017**, 13, 1702240.
- [17] D. J. Dietzen, in *Principles and Applications of Molecular Diagnostics*, (Eds: N. Rifai, A. R. Horvath, C. T. Wittwer), Elsevier, New York **2018**, p. 345.
- [18] L. Eisoltd, A. Smith, T. Scheibel, *Mater. Today* **2011**, 14, 80.
- [19] K. Gellynck, P. C. M. Verdonk, E. Van Nimmen, K. F. Almqvist, T. Gheysens, G. Schoukens, L. Van Langenhove, P. Kiekens, J. Mertens, G. Verbruggen, *J. Mater. Sci.: Mater. Med.* **2008**, 19, 3399.
- [20] M. Hofer, G. Winter, J. Myschik, *Biomaterials* **2012**, 33, 1554.
- [21] G. Lang, S. Jokisch, T. Scheibel, *J. Visualized Exp.* **2013**, 75, 50492.
- [22] J. Gosline, P. Guerette, C. Ortlepp, K. Savage, *J. Exp. Biol.* **1999**, 202, 3295.
- [23] Y. Wang, D. D. Rudym, A. Walsh, L. Abrahamsen, H.-J. Kim, H. S. Kim, C. Kirker-Head, D. L. Kaplan, *Biomaterials* **2008**, 29, 3415.
- [24] A. Leal-Egaña, T. Scheibel, *Biotechnol. Appl. Biochem.* **2010**, 55, 155.
- [25] S. Wright, S. L. Goodacre, *BMC Res. Notes* **2012**, 5, 326.
- [26] F. Maeder, *Text. tintes Mediterr. época romana* **2008**, 112.
- [27] E. Morgan, *J. Des. Hist.* **2016**, 29, 8.
- [28] A. Gell, *Anthropol. Today* **1988**, 4, 6.
- [29] S. J. Vainker, *Chinese Silk: A Cultural History*, Rutgers University Press, New Brunswick, NJ **2004**.
- [30] S. Arcidiacono, C. Mello, D. Kaplan, S. Cheley, H. Bayley, *Appl. Microbiol. Biotechnol.* **1998**, 49, 31.
- [31] F. Bauer, T. Scheibel, *Angew. Chem., Int. Ed.* **2012**, 51, 6521.
- [32] J. Shi, S. Lua, N. Du, X. Liu, J. Song, *Biomaterials* **2008**, 29, 2820.
- [33] T. B. Aigner, E. DeSimone, T. Scheibel, *Adv. Mater.* **2018**, 30, 1704636.
- [34] T. D. Sutherland, J. H. Young, S. Weisman, C. Y. Hayashi, D. J. Merritt, *Annu. Rev. Entomol.* **2010**, 55, 171.
- [35] T. D. Sutherland, S. Weisman, A. A. Walker, S. T. Mudie, *Biopolymers* **2012**, 97, 446.
- [36] Y. Shen, M. A. Johnson, D. C. Martin, *Macromolecules* **1998**, 31, 8857.
- [37] L. Römer, T. Scheibel, *Prion* **2008**, 2, 154.
- [38] S. Sukigara, M. Gandhi, J. Ayutsede, M. Micklus, F. Ko, *Polymer* **2003**, 44, 5721.
- [39] U.-J. Kim, J. Park, C. Li, H.-J. Jin, R. Valluzzi, D. L. Kaplan, *Biomacromolecules* **2004**, 5, 786.
- [40] C. Jiang, X. Wang, R. Gunawidjaja, Y. H. Lin, M. K. Gupta, D. L. Kaplan, R. R. Naik, V. V. Tsukruk, *Adv. Funct. Mater.* **2007**, 17, 2229.
- [41] O. N. Tretinnikov, Y. Tamada, *Langmuir* **2001**, 17, 7406.
- [42] I. C. Um, C. S. Ki, H. Kweon, K. G. Lee, D. W. Ihm, Y. H. Park, *Int. J. Biol. Macromol.* **2004**, 34, 107.
- [43] M. M. R. Khan, H. Morikawa, Y. Gotoh, M. Miura, Z. Ming, Y. Sato, M. Iwasa, *Int. J. Biol. Macromol.* **2008**, 42, 264.
- [44] R. Nazarov, H.-J. Jin, D. L. Kaplan, *Biomacromolecules* **2004**, 5, 718.
- [45] A. P. Kiseleva, P. V. Krivoschapkin, E. F. Krivoschapkina, *Front. Chem.* **2020**, 8, 554.
- [46] R. Lewis, *BioScience* **1996**, 46, 636.
- [47] S. Kumari, G. Lang, E. DeSimone, C. Spengler, V. T. Trossmann, S. Lücker, M. Hudel, K. Jacobs, N. Krämer, T. Scheibel, *Data Brief* **2020**, 32, 106305.
- [48] S. Winkler, S. Szela, P. Avtges, R. Valluzzi, D. A. Kirschner, D. Kaplan, *Int. J. Biol. Macromol.* **1999**, 24, 265.
- [49] M. Humenik, M. Mohrand, T. Scheibel, *Bioconjugate Chem.* **2018**, 29, 898.
- [50] E. Bini, C. W. P. Foo, J. Huang, V. Karageorgiou, B. Kitchel, D. L. Kaplan, *Biomacromolecules* **2006**, 7, 3139.
- [51] K. Numata, J. Hamasaki, B. Subramanian, D. L. Kaplan, *J. Controlled Release* **2010**, 146, 136.
- [52] H. M. Herold, T. B. Aigner, C. E. Grill, S. Krüger, A. Taubert, T. Scheibel, *Bioinspired, Biomimetic Nanobiomater.* **2019**, 8, 99.
- [53] H. A. Currie, O. Deschaume, R. R. Naik, C. C. Perry, D. L. Kaplan, *Adv. Funct. Mater.* **2011**, 21, 2889.
- [54] J. Liu, D. Guo, Y. Zhou, Z. Wu, W. Li, F. Zhao, X. Zheng, *J. Archaeol. Sci.* **2011**, 38, 1763.
- [55] T. Scheibel, H. Zahn, A. Krasowski, in *Ullmann's Encyclopedia of Industrial Chemistry*, Wiley, Weinheim, **2016**, p. 1.
- [56] S. Bera, S. P. Mondal, D. Naskar, S. C. Kundu, S. K. Ray, *Org. Electron.* **2014**, 15, 1767.
- [57] N. Gogurla, S. C. Kundu, S. K. Ray, *Nanotechnology* **2017**, 28, 145202.
- [58] R. K. Pal, S. C. Kundu, V. K. Yadavalli, *ACS Appl. Mater. Interfaces* **2018**, 10, 9620.
- [59] N. Qi, B. Zhao, S.-D. Wang, S. S. Al-Deyab, K.-Q. Zhang, *RSC Adv.* **2015**, 5, 50878.
- [60] J. D. Ryan, D. A. Mengistie, R. Gabrielsson, A. Lund, C. Müller, *ACS Appl. Mater. Interfaces* **2017**, 9, 9045.
- [61] S. Takamatsu, T. Lonjaret, E. Ismailova, A. Masuda, T. Itoh, G. G. Malliaras, *Adv. Mater.* **2016**, 28, 4485.
- [62] F. He, X. You, H. Gong, Y. Yang, T. Bai, W. Wang, W. Guo, X. Liu, M. Ye, *ACS Appl. Mater. Interfaces* **2020**, 12, 6442.
- [63] W. Lu, P. Yu, M. Jian, H. Wang, H. Wang, X. Liang, Y. Zhang, *ACS Appl. Mater. Interfaces* **2020**, 12, 11825.
- [64] J.-H. Choi, W. Xie, Y. Gu, C. D. Frisbie, T. P. Lodge, *ACS Appl. Mater. Interfaces* **2015**, 7, 7294.
- [65] M. Kaltenbrunner, G. Adam, E. D. Głowacki, M. Drack, R. Schwödiauer, L. Leonat, D. H. Apaydin, H. Groiss, M. C. Scharber, M. S. White, N. S. Sariciftci, S. Bauer, *Nat. Mater.* **2015**, 14, 1032.
- [66] T. P. Lodge, T. Ueki, *Acc. Chem. Res.* **2016**, 49, 2107.
- [67] J. Zhao, Z. Chi, Z. Yang, X. Chen, M. S. Arnold, Y. Zhang, J. Xu, Z. Chi, M. P. Aldred, *Nanoscale* **2018**, 10, 5764.
- [68] M. Kang, H.-J. Jin, *Colloid Polym. Sci.* **2007**, 285, 1163.
- [69] C. Shi, J. Wang, M. L. Sushko, W. Qiu, X. Yan, X. Y. Liu, *Adv. Funct. Mater.* **2019**, 29, 1904777.
- [70] R. Ranjana, N. Parushuram, K. S. Harisha, S. Asha, B. Narayana, M. Mahendra, Y. Sangappa, *J. Mater. Sci.: Mater. Electron.* **2020**, 31, 249.
- [71] C. Müller, M. Hamedi, R. Karlsson, R. Jansson, R. Marcilla, M. Hedhammar, O. Inganäs, *Adv. Mater.* **2011**, 23, 898.
- [72] Z. Yin, M. Jian, C. Wang, K. Xia, Z. Liu, Q. Wang, M. Zhang, H. Wang, X. Liang, X. Liang, Y. Long, X. Yu, Y. Zhang, *Nano Lett.* **2018**, 18, 7085.
- [73] S. C. Narayanan, K. R. Karpagam, A. Bhattacharyya, *Fibers Polym.* **2015**, 16, 1269.
- [74] Y. Guo, M. T. Otley, M. Li, X. Zhang, S. K. Sinha, G. M. Treich, G. A. Sotzing, *ACS Appl. Mater. Interfaces* **2016**, 8, 26998.
- [75] A. Lund, S. Darabi, S. Hultmark, J. D. Ryan, B. Andersson, A. Ström, C. Müller, *Adv. Mater. Technol.* **2018**, 3, 1800251.
- [76] A. T. N. Dao, K. Nakayama, J. Shimokata, T. Taniike, *Polym. Chem.* **2017**, 8, 1049.
- [77] A. Martel, M. Burghammer, R. J. Davies, C. Riekel, *Biomacromolecules* **2007**, 8, 3548.

- [78] K. Spiess, R. Ene, C. D. Keenan, J. Senker, F. Kremer, T. Scheibel, *J. Mater. Chem.* **2011**, *21*, 13594.
- [79] D. Na, J. Choi, J. Lee, J. W. Jeon, B. H. Kim, *ACS Appl. Mater. Interfaces* **2019**, *11*, 27353.
- [80] K. Spiess, A. Lammel, T. Scheibel, *Macromol. Biosci.* **2010**, *10*, 998.
- [81] M. Liu, Y. Zhang, K. Liu, G. Zhang, Y. Mao, L. Chen, Y. Peng, T. H. Tao, *Adv. Mater.* **2021**, *33*, 2004733.
- [82] S. Tsukada, H. Nakashima, K. Torimitsu, *PLoS One* **2012**, *7*, e33689.
- [83] H. Zhang, J. Zhao, T. Xing, S. Lu, G. Chen, *Polymers* **2019**, *11*, 1774.
- [84] A. Reizabal, S. Gonçalves, R. Brito-Pereira, P. Costa, C. M. Costa, L. Pérez-Álvarez, J. L. Vilas-Vilela, S. Lanceros-Méndez, *Nanoscale Adv.* **2019**, *1*, 2284.
- [85] S. Salehi, K. Koeck, T. Scheibel, *Molecules* **2020**, *25*, 737.
- [86] I. Statistics, *International Energy Agency, Key World Energy Statistics 2020*, Paris **2020**, [https://www.petrofed.be/sites/default/files/editor/Key\\_World\\_Energy\\_Statistics\\_2020\\_0.pdf](https://www.petrofed.be/sites/default/files/editor/Key_World_Energy_Statistics_2020_0.pdf) (accessed: November 2020).
- [87] P. E. Shaw, *Proc. R. Soc. London, Ser. A* **1917**, *94*, 16.
- [88] F.-R. Fan, Z.-Q. Tian, Z. L. Wang, *Nano Energy* **2012**, *1*, 328.
- [89] Z. L. Wang, *ACS Nano* **2013**, *7*, 9533.
- [90] H.-J. Kim, J.-H. Kim, K.-W. Jun, J.-H. Kim, W.-C. Seung, O. H. Kwon, J.-Y. Park, S.-W. Kim, I.-K. Oh, *Adv. Energy Mater.* **2016**, *6*, 1502329.
- [91] C. Liu, J. Li, L. Che, S. Chen, Z. Wang, X. Zhou, *Nano Energy* **2017**, *41*, 359.
- [92] T. Ikeda, *Fundamentals of Piezoelectricity*, Oxford University Press, Oxford, UK **1996**.
- [93] E. N. Harvey, *Science* **1939**, *89*, 460.
- [94] S. K. Ghosh, D. Mandal, *Appl. Phys. Lett.* **2016**, *109*, 103701.
- [95] S. K. Ghosh, D. Mandal, *Nano Energy* **2016**, *28*, 356.
- [96] B. Y. Lee, J. Zhang, C. Zueger, W.-J. Chung, S. Y. Yoo, E. Wang, J. Meyer, R. Ramesh, S.-W. Lee, *Nat. Nanotechnol.* **2012**, *7*, 351.
- [97] T. Huang, Y. Zhang, P. He, G. Wang, X. Xia, G. Ding, T. H. Tao, *Adv. Mater.* **2020**, *32*, 1907336.
- [98] S. Paria, R. Bera, S. K. Karan, A. Maitra, A. K. Das, S. K. Si, L. Halder, A. Bera, B. B. Khatua, *ACS Appl. Energy Mater.* **2018**, *1*, 4963.
- [99] Y. Guo, X.-S. Zhang, Y. Wang, W. Gong, Q. Zhang, H. Wang, J. Brugger, *Nano Energy* **2018**, *48*, 152.
- [100] Q. Zheng, L. Fang, H. Guo, K. Yang, Z. Cai, M. A. B. Meador, S. Gong, *Adv. Funct. Mater.* **2018**, *28*, 1706365.
- [101] W. Sparreboom, A. van den Berg, J. C. Eijkel, *Nat. Nanotechnol.* **2009**, *4*, 713.
- [102] W. Xin, Z. Zhang, X. Huang, Y. Hu, T. Zhou, C. Zhu, X.-Y. Kong, L. Jiang, L. Wen, *Nat. Commun.* **2019**, *10*, 3876.
- [103] J. Chen, W. Xin, X.-Y. Kong, Y. Qian, X. Zhao, W. Chen, Y. Sun, Y. Wu, L. Jiang, L. Wen, *ACS Energy Lett.* **2020**, *5*, 742.
- [104] Z. Zhang, S. Yang, P. Zhang, J. Zhang, G. Chen, X. Feng, *Nat. Commun.* **2019**, *10*, 2920.
- [105] A. Mardiana-Idayu, S. Riffat, *Renewable Sustainable Energy Rev.* **2012**, *16*, 1241.
- [106] P. M. Cuce, S. Riffat, *Renewable Sustainable Energy Rev.* **2015**, *47*, 665.
- [107] H.-P. Zhao, X.-Q. Feng, S.-W. Yu, W.-Z. Cui, F.-Z. Zou, *Polymer* **2005**, *46*, 9192.
- [108] J. Zhang, R. Rajkhowa, J. Li, X. Y. Liu, X. G. Wang, *Mater. Des.* **2013**, *49*, 842.
- [109] J. S. Ishay, V. Barenholz-Paniry, *J. Insect Physiol.* **1995**, *41*, 753.
- [110] B. Tulachan, S. K. Meena, R. K. Rai, C. Mallick, T. S. Kusrkar, A. K. Teotia, N. K. Sethy, K. Bhargava, S. Bhattacharya, A. Kumar, R. K. Sharma, N. Sinha, S. K. Singh, M. Das, *Sci. Rep.* **2014**, *4*, 5434.
- [111] J. Ishay, F. Ruttner, *Z. Vgl. Physiol.* **1971**, *72*, 423.
- [112] J. S. Ishay, A. Ben-Shalom, *Physiol. Chem. Phys. Med. NMR* **1992**, *24*, 323.
- [113] Q. Zhang, X. F. Xiao, G. Wang, X. Ming, X. H. Liu, H. Wang, H. J. Yang, W. L. Xu, X. B. Wang, *J. Mater. Chem. A* **2018**, *6*, 17212.
- [114] K. Schmidt-Rohr, *J. Chem. Educ.* **2015**, *92*, 2094.
- [115] P. Jean-Baptiste, R. Ducroux, *Energy Policy* **2003**, *31*, 155.
- [116] T. R. Karl, K. E. Trenberth, *Science* **2003**, *302*, 1719.
- [117] J. A. Sathaye, N. H. Ravindranath, *Annu. Rev. Energy Environ.* **1998**, *23*, 387.
- [118] R. E. H. Sims, *Sol. Energy* **2004**, *76*, 9.
- [119] G. A. S. Edwards, *WIREs Clim. Change* **2019**, *10*, e607.
- [120] P. Lauri, P. Havlik, G. Kindermann, N. Forsell, H. Böttcher, M. Obersteiner, *Energy Policy* **2014**, *66*, 19.
- [121] Y. Sribna, O. Trokhymets, I. Nosatov, I. Kriukova, *E3S Web Conf.* **2019**, *123*, 01044.
- [122] C. H. Haustein, in *The Gale Encyclopedia of Science*, (Eds: K. L. Lerner, B. W. Lerner), Gale, Farmington Hills, MI **2014**.
- [123] M. Borghei, J. Lehtonen, L. Liu, O. J. Rojas, *Adv. Mater.* **2018**, *30*, 1703691.
- [124] C. Guo, R. Hu, W. Liao, Z. Li, L. Sun, D. Shi, Y. Li, C. Chen, *Electrochim. Acta* **2017**, *236*, 228.
- [125] X. Zhu, E. Aoyama, A. V. Birk, O. Onasanya, W. H. Carr, L. Mouroukh, S. D. Minter, M. Vittadello, *Biochim. Biophys. Acta, Bioenerg.* **2020**, *1861*, 148262.
- [126] W. Yang, L. Lv, X. Li, X. Han, M. Li, C. Li, *ACS Nano* **2020**, *14*, 10600.
- [127] C. Wang, K. Xia, Y. Zhang, D. L. Kaplan, *Acc. Chem. Res.* **2019**, *52*, 2916.
- [128] L. Zhou, P. Fu, X. Cai, S. Zhou, Y. Yuan, *Appl. Catal., B* **2016**, *188*, 31.
- [129] T. D. Rapson, *Molecules* **2016**, *21*, 919.
- [130] T. D. Rapson, T. D. Sutherland, J. S. Church, H. E. Trueman, H. Dacres, S. C. Trowell, *ACS Biomater. Sci. Eng.* **2015**, *1*, 1114.
- [131] C. Acar, *Int. J. Energy Res.* **2018**, *42*, 3732.
- [132] R. B. Kaunda, *J. Energy Nat. Resour. Law* **2020**, *38*, 237.
- [133] W. Liu, D. B. Agusdinata, S. W. Myint, *Int. J. Appl. Earth Obs. Geoinf.* **2019**, *80*, 145.
- [134] K. S. Wu, Y. Hu, Z. L. Cheng, P. Pan, L. Y. Jiang, J. T. Mao, C. K. Ni, X. F. Gu, Z. X. Wang, *J. Membr. Sci.* **2019**, *592*, 8.
- [135] J. Hou, C. Cao, F. Idrees, X. Ma, *ACS Nano* **2015**, *9*, 2556.
- [136] K. S. Poonam, A. Arora, S. K. Tripathi, *J. Energy Storage* **2019**, *21*, 801.
- [137] I. Chotia, S. Chowdhury, presented at 2015 IEEE Innovative Smart Grid Technol. – Asia (ISGT ASIA), Bangkok, Thailand November **2015**.
- [138] Y. J. Kim, Y. Abe, T. Yanagiura, K. C. Park, M. Shimizu, T. Iwazaki, S. Nakagawa, M. Endo, M. S. Dresselhaus, *Carbon* **2007**, *45*, 2116.
- [139] H. Luo, M. Chen, J. Cao, M. Zhang, S. Tan, L. Wang, J. Zhong, H. Deng, J. Zhu, B. Lu, *Nano-Micro Lett.* **2020**, *12*, 113.
- [140] Y. X. Wang, Y. F. Song, Y. Wang, X. Chen, Y. Y. Xia, Z. Z. Shao, *J. Mater. Chem. A* **2015**, *3*, 773.
- [141] Y. S. Yun, S. Y. Cho, H. J. Jin, *Macromol. Res.* **2014**, *22*, 509.
- [142] P. Ma, Y. Lou, S. Cong, Z. Lu, K. Zhu, J. Zhao, G. Zou, *Adv. Energy Mater.* **2020**, *10*, 1903357.
- [143] Q. Dong, Y. Fang, Y. Shao, P. Mulligan, J. Qiu, L. Cao, J. Huang, *Science* **2015**, *347*, 967.
- [144] W.-Q. Liao, Y. Zhang, C.-L. Hu, J.-G. Mao, H.-Y. Ye, P.-F. Li, S. D. Huang, R.-G. Xiong, *Nat. Commun.* **2015**, *6*, 7338.
- [145] Q. Pan, Z.-B. Liu, Y.-Y. Tang, P.-F. Li, R.-W. Ma, R.-Y. Wei, Y. Zhang, Y.-M. You, H.-Y. Ye, R.-G. Xiong, *J. Am. Chem. Soc.* **2017**, *139*, 3954.
- [146] Y.-M. You, W.-Q. Liao, D. Zhao, H.-Y. Ye, Y. Zhang, Q. Zhou, X. Niu, J. Wang, P.-F. Li, D.-W. Fu, Z. Wang, S. Gao, K. Yang, J.-M. Liu, J. Li, Y. Yan, R.-G. Xiong, *Science* **2017**, *357*, 306.
- [147] Z. Lu, H. Zhang, C. Mao, C. M. Li, *Appl. Energy* **2016**, *164*, 57.
- [148] S. Lee, S. H. Kim, Y.-Y. Jo, W.-T. Ju, H.-B. Kim, H. Kweon, *Biomolecules* **2021**, *11*, 70.



**Stephen Strassburg** has a Bachelor's degree in Chemical Engineering from Northeastern University and a Ph.D. in Polymer Science and Engineering from University of Massachusetts—Amherst. He is currently doing his Post-Doc at the Universität Bayreuth in Germany.



**Shakir Zainuddin** has a Bachelor's degree in Process and Environmental Engineering from HTWG Konstanz and Master's degree in Biofabrication from Universität Bayreuth. He is currently doing a Ph.D. in the Department of Biomaterials at Universität Bayreuth.



**Thomas Scheibel** has been Full Professor at the Department of Biomaterials at the Universität Bayreuth in Germany since 2007. He received both his Diploma of Biochemistry (1994) and a Dr. rer. nat. (1998) from the Universität Regensburg in Germany. After his Postdoc at the University of Chicago (1998–2001), he received his habilitation (2007) from the Technische Universität München in Germany. His research focuses on biotechnological production and processing of structural proteins, as well as their biomedical and technical application thereof.